Cite Information for this article:

Omoregie, A.I., Muda, K., Bakri, M.K.B. *et al.* Calcium carbonate bioprecipitation mediated by ureolytic bacteria grown in pelletized organic manure medium. *Biomass Conv. Bioref.* (2022). **https://doi.org/10.1007/s13399-022-03239-w**

Calcium carbonate bioprecipitation mediated by ureolytic bacteria grown in pelletised organic manure medium

Armstrong Ighodalo Omoregie[a,*], Khalida Muda[a], Muhammad Khusairy Bin Bakri[b], Md Rezaur Rahman[c], Fahmi Asyadi Md Yusof[d], and Oluwapelumi Olumide Ojuri[e]

[a]Department of Water and Environmental Engineering, School of Civil Engineering, Faculty of Engineering, Universiti Teknologi Malaysia, 81310 Skudai, Johor, Malaysia.

[b]Composites Materials and Engineering Center, Washington State University, 2001 East Grimes Way, Pullman, WA, 99164, United States.

[c]Department of Chemical Engineering and Energy Sustainability, Faculty of Engineering, Universiti Malaysia Sarawak, Jalan Datuk Mohammad Musa, 94300 Kota Samarahan, Sarawak, Malaysia

[d]Malaysian Institute of Chemical and Bioengineering Technology, Universiti Kuala Lumpur, Alor Gajah 78000, Melaka, Malaysia

[e]Built Environment and Sustainable Technologies (BEST) Research Institute, Liverpool John Moores University, Liverpool L3 3AF, United Kingdom.

[*]**Corresponding Author:**

Armstrong Ighodalo Omoregie, Post-Doctoral Researcher, Department of Water and Environmental Engineering, School of Civil Engineering, Faculty of Engineering, Universiti Teknologi Malaysia, 81310 Skudai, Johor, Malaysia. Emails: adaloomoregie@gmail.com; ioarmstrong@utm.my; ORCID: 0000-0002-6356-9638

ABSTRACT

New sustainable methods utilizing biological processes to mediate the improvement of soil properties have recently emerged. Microbially induced calcite precipitation (MICP) has been demonstrated as a potential sustainable technique for soil improvement and solidification, erosion control and prevention, and remediation of contaminants. This paper describes experiments conducted to demonstrate the efficacy of using pelletised organic manure (POM), supplemented with varying concentrations of yeast extract (20% to 80%, w/v) as a suitable alternative low-cost nutrient source for bacteria cultivation during the MICP soil biocementation process. The evaluation entails using scanning electron microscopy with electron dispersive X-ray spectroscopy (SEM-EDS), Fourier-transform infrared spectroscopy (FTIR), differential scanning calorimetry (DSC), and thermogravimetric analysis (TGA) analysis for the evaluation of cementation efficiency, relative merits of the mechanisms and biocementation byproduct. The results demonstrated that ureolytic bacteria can be cultivated with POM that contains yeast extract ranging from 4 g/L to 8 g/L and this alternative bacteria cultivation nutrient source produced more crystal formations with less visible pore spaces in biocemented soil. This study reveals that more treatment cycles (bacterial cultures and chemical solution) approach would be required during biocementation to achieve successful crystal shapes to bridge soil particles when using ureolytic bacteria grown in the inexpensive medium supplemented with low yeast extract.

Keywords: Nutrient source; Pelletised dairy manure; Calcium carbonate; Morphology; Ureolysis; Sporosarcina pasteurii

1. Introduction

The biomineralisation process via metabolic activities has been dramatically shown in literature for its potential usefulness in engineering and biotechnological practices. In the past three decades, the scientific community has increasingly focused its attention on microbially induced calcite precipitation (MICP), a biologically induced mineralization process. Out of the several MICP methods/techniques (including photosynthesis, ureolysis (urea hydrolysis), sulphate reduction, ammonification, and denitrification (nitrate reduction), ureolysis appears to be the most straightforward pathway for microorganisms to manipulate their environmental conditions and precipitate carbonate polymorphs [1]. MICP application primarily focuses on soil solidification/enhancement and heavy metal remediation/removal. The literature has suggested that siderophores and indole-3-acetic acid are secreted by ureolytic bacteria (i.e., *Staphylococcus equorum*, *Lysinibacillus* sp., and *Pseudochrobactrum* sp.), can help accelerate plant development and increase plant tolerance to heavy metals during MICP process [2]. Furthermore, contaminated soils containing heavy metal ions are then sequestrated into stable mineral forms through biocementation treatment, which helps minimize metal mobility/toxicity and increases soil strength.

Under the ureolysis-driven MICP process, urea substrate is hydrolyzed by urease from the bacterial cells, which leads to the breakdown into ammonia (NH_3) and carbamate (NH_2COOH) ([3]. This is followed by immediate hydrolysis to produce NH_3 and carbonic acid (H_2CO_3) [4]. The NH_3 later forms ammonium ion (NH_4^+) and hydroxide ion (H^+), then also NH_2COOH results in bicarbonate (HCO_3^-) ions. During the MICP process, the pH level of the solution increases to alkaline due to hydroxide ions which causes a shift in the HCO_3^- equilibrium. This leads to the carbonate (CO_3^{-2}) ions formation. When a calcium (Ca^+) source such as calcium chloride ($CaCl_2$) is introduced or present in the solution, the Ca^+ ions bind with CO_3^{-2} to form calcium carbonate ($CaCO_3$) crystal precipitation [1]. $CaCl_2$ is the most often utilized calcium source in MICP technological capabilities because it can produce CaCO3, which has a high amount of precipitation and is thermodynamically stable [5,6].

Sporosarcina pasteurii (previously known as *Bacillus pasteurii*) is one of the highest urease-producing and calcifying bacteria compared to other microorganisms. It is Gram-positive, alkaliphilic, non-pathogenic, and has the propensity to generate endospores for survival in harsh environments [7]. The MICP has been demonstrated under various conditions (such as laboratory-scale, pilot-scale, and field-scale) as a potential sustainable technique for soil improvement and solidification [8–11], erosion control and prevention [12–14], and remediation of contaminants (such as copper, cadmium, and mercy) [15–17].

MICP viability is determined not only by technical features of treatment circumstances but also by economic obstacles. The material cost of the required substances/chemicals is one of the most challenging

difficulties in determining the process's overall feasibility [10]. Microorganisms require nutrients for propagation and metabolic functions. However, the nutrients needed for microbial growth contribute to a substantial portion of total expenses that ranges up to 60% in the MICP process [18,19]. The elements available in these nutrients can influence bacterial activity and the reproduction rate of $CaCO_3$ induced by the ureolytic bacteria [20]. Due to the enormous cost of bacterial cultivation for large-scale implementation, the present investigations on MICP have been mostly restricted to a limited laboratory-scale [21]. To reduce costs, the expensive protein-rich cultivation medium such as yeast extract has been widely discussed in the literature to identify alternative nutrient sources. In recent years, scholars have reported the potential usefulness of inexpensive food-grade yeast extract, kitchen waste medium, soybean, and corn steep liquor to grow ureolytic bacterial cells for $CaCO_3$ precipitation [14,19,22,23].

To overcome the challenge of costly bacterial production to induce $CaCO_3$ precipitation at a large scale, this paper offers an efficient and economical technique to cultivate alternative nutrient sources for considerable soil improvement. For bacterial propagation, some nutritional components known as macronutrients (i.e., carbon, nitrogen, and potassium) are required in greater abundance, while only traces of micronutrients (i.e., manganese, zinc, molybdenum, nickel) are required. Macronutrients are often supplemented from a natural source. In contrast, micronutrient requirements are met by traces of elements present as contaminants in the water or waste nutrients used for the medium preparation [1]. Waste materials (i.e., dairy farmland, Fish waste, rice straw) can serve as nutritional resources to cultivate numerous microbial species for promising biotechnological or engineering applications [24,25].

Organic manure is an agricultural waste that is used as a low-cost feedstock available around the world. Hence, this present study aimed to determine the effect of using inexpensive pelletised organic manure (POM) medium supplemented with varying concentrations of yeast extract for soil biocementation. The effective usage of organic manure sourced from local dairy farmland was considered a nutritional source for ureolytic bacterial productivity. The feasibility to absorb nutrients from the waste medium was evaluated/monitored. This study also determined the effect of various temperatures and concentrations of treatment ingredients on MICP. Upon completion of the biocementation treatment test, the soil samples were evaluated with scanning electron microscopy with electron dispersive X-ray spectroscopy (SEM-EDS), Fourier-transform infrared spectroscopy (FTIR), differential scanning calorimetry (DSC), and thermogravimetric analysis (TGA) analysis.

2. Materials and methods

2.1. Raw material

Pelletized organic manure as shown in **Fig. 1** was purchased (US$ 1.4 per 1 kg) locally from a dairy farm supplier situated in Agricultural & Industrial Chemical Trading, Jalan Buso, Bau, Sarawak, Malaysia) to serve as an alternative nutrient source for bacterial cultivation. Physiochemical analyses of the organic material (**Table 1**) were performed to determine the chemical compounds following the testing methods for fertilizers [26]. The X-ray fluorescence analysis of POM was carried out to determine the elemental composition of materials (**Table 2**) using a wavelength-dispersive X-ray fluorescence spectrometer (WDX-4000, China) following the ASTM E1621-21 [27] standard.

2.2. Microorganisms and culture conditions

For this present MICP study, the ureolytic bacterium *Sporosarcina pasteurii* (DSM 33 type strain) was purchased from The Leibniz Institute DSMZ - German Collection of Microorganisms and Cell Cultures GmbH (Braunschweig, Germany) and used throughout this paper. The non-pathogenic microorganism was received in lyophilized powdered form and reactivated in a Petri dish containing freshly prepared nutrient agar (28 g/L, HiMedia, Laboratories Pvt. Ltd., India). Colonies of the bacterium were cultivated under aerobic conditions using a sterile 13 g/L of nutrient broth (Himedia Laboratories Pvt. Ltd., India), 10 g/L of ammonium chloride, and 20 g/L of urea (Merck, Darmstadt, Germany). The medium initial pH was adjusted to 8.0 by 1 M of NaOH (Sigma Aldrich, Malaysia) and HCl (Sigma Aldrich, Malaysia) before sterilization at 121 $^{\circ}$C using an autoclave machine (Hirayama-110, Kasukabe-Shi Saitama, Japan). The ureolytic microorganism was then grown to an early stationary phase (24 h incubation at 32 $^{\circ}$C) with a rotation rate of 150 rpm until the liquid culture became turbid. Afterwards, the ureolytic bacterial cultures were stored at 4 $^{\circ}$C for no longer than a month for subsequent use [28]. All the chemicals and reagents used in this current study were of analytical grade, except for the food-grade (low-purity) yeast extract.

2.3. Preparation of an alternative nutrient source for bacterial cultivation

Ureolytic bacteria require abundant energy sources for cell growth and urease production to enable biomineral precipitation. The POM was investigated in this paper to serve as a cheap alternative medium with sufficient organic nutrients capable of supporting microbial propagation. The material (500 g) was crushed into powdered form before being used to prepare the culture medium. In a beaker (10000 mL capacity), 200 g of the powdered material, 0.17 M of sodium acetate (HiMedia Laboratories Pvt. Ltd., India), and 0.0125 M of ammonium chloride

(HiMedia Laboratories Pvt. Ltd., India) were placed, followed by 1 L of deionised water. Sodium acetate is typically added into the medium to serve as a carbon source and facilitate or improve the ureolytic bacterial cell growth [7,29]. To promote an ammonium-rich environment for the ureolytic bacteria, ammonium ions such as ammonium chloride are added to the growth medium [30]. Also, ammonium chloride has been reported to help stimulate the MICP process, especially during the biocementation treatment phase [31]. The solution was placed heated on a hot plate for 15 min and transferred into a clean Schott bottle. The undesired substances that did not dissolve during heating were subsequently removed by simple filtration and separation method using a Whatman filter paper® (grade number 1). The growth medium was then autoclaved, while urea (40 g/L, Merck, Shd. Bhd., Malaysia) was later introduced (by 0.45 μm filter sterilisation) after the medium cooled to room temperature (26 $^{\circ}$C). The prepared POM medium has a neutral pH level of 6.8, and the initial pH level was not adjusted. A preliminary study (data not shown) indicated that the prepared growth medium could only achieve an absorbance reading of 0.2 but increased to 0.4 when yeast extract was supplemented into the medium. Hence, in this study, four bacterial inoculum solutions were prepared using different medium constituents depending on the added concentration of yeast extract (Angel Yeast Co. Ltd., China). Yeast extract is a rich source of organic nitrogen, amino acids, vitamins, minerals, and peptides which can promote sufficient microbial growth [7,13]. Hence, a low-cost yeast extract was introduced to support bacterial growth. The four prepared mediums constituted the ingredients previously mentioned, except growth medium-1 (GM-1, which contained 8 g/L of yeast extract); growth medium-2 (GM-2, which had 6 g/L of yeast extract); growth medium -3 (GM-3, which included 4 g/L of yeast extract); and growth medium-4 (GM-4, which contained 2 g/L of yeast extract). All mediums were then transferred into different sterile shake flasks and inoculated with 10% (v/v) of starter culture containing *Sporosarcina pasteurii*. The flasks were then incubated in an incubator shaker (CERTOMAT® CT plus Sartorius, Germany) for 24 h at 32 $^{\circ}$C with shaking conditions (150 rev/min). At the end of the cultivation phase, the culture flasks (**Fig. 2**) were then used for subsequent experiments.

2.4. *Monitoring of growth profile, pH profile, and urease activity*

Bacterial biomass was measured to determine the bacterial cell density (also known as optical density) at a wavelength of 600 nm (OD_{600}) using a spectrophotometer (Thermo ScientificTM GENESYSTM 20, United States). The turbidity of the bacterial growth medium was proportional to the quantity of microorganisms present (either viable or dead cells) [32]. Hence, A higher turbidity level suggested a more significant number of microbial cells. Before biomass assessment, the spectrophotometer was calibrated using blank samples (un-inoculated

freshly prepared growth medium). On the other hand, the pH meter (SevenEasyTM–Mettler Toledo, Malaysia) was calibrated in buffer solutions (pH, 4, 7, and 10, Sigma-Aldrich Sdn. Bhd., Malaysia) before measuring the pH acidity or alkalinity profile of the bacterial cultures. The obtained OD_{600} and pH values were used to plot the bacterial cell's respective growth and pH profiles after being grown/studied in a POM medium for 24 h.

The urease activity of *Sporosarcina pasteurii* was determined through relative conductivity change after being grown in the proposed medium (GM-1 to GM4) for 24 h. The probe in a benchtop conductivity meter (Milwaukee MI806, United States) was used to measure the relative conductivity changes of the mixture which contained 10 mL of bacterial culture and 90 mL of urea solution (1.11 M) for 5 min at 25 ± 2 ^{o}C. The conductivity rate change (mS.cm/min), was determined, taking into around the dilution factor (10) before being converted into the urease activity (mM urea hydrolysed/min) [33]. One unit of urease activity is defined in the measured range of activities as the amount of enzyme that catalyses the breakdown of 1 mM of urea per minute [34].

2.5. *Biomineralization test*

A series of experiments were conducted to measure the rate of precipitates induced by ureolytic bacterial cells. Two factors were selected for this study: (i) the effect of cementation treatment ingredients at different concentrations; and (ii) the effect of temperature as an environmental condition. The mass of precipitates and pH effluents were measured and used to evaluate the impact of varying chemical concentrations and temperatures on the performance of MICP by *S. pasteurii*. This study provided analytical grade urea (Merck, Shd. Bhd., Malaysia) and calcium chloride (Lianyungang Longyi Industry Co. Ltd., China) cementation constituents for the biomineralisation test via the MICP process. Since it has been reported that the optimal molar ratio of urea and Calcium ions was 1:1 [10,12], hence equimolar of each substance (urea and $CaCl_2$) were used in this paper. The chemicals were prepared in Schott bottles (1 L) containing sterile deionised water. Urea and calcium chloride were sterilised via ultraviolet light in a biological safety cabinet (Thermofisher Scientific, 1300 series A2, USA). After cooling to room temperature, the chemicals were later added to the Schott bottles containing the sterilised deionized water.

For the effect of cementation treatment ingredients at different concentrations, equimolar solutions of $CaCl_2$-urea were formulated at 0.25 M, 0.5 M, 0.75 M, 1.0 M, and 1.5 M, respectively, and incubated (Incucell 55-Eco Line, MMM Medcenter Einrichtungen Gmb, Germany) at 32 $^{\circ}$C for 72 hr. On the other hand, the effect of varying temperatures, ranging from 10 ^{o}C and 50 ^{o}C (at an interval of 10^{o}C) equimolar of $CaCl_2$-urea (1 M), was selected. All the samples were incubated without shaking, and control samples (without bacteria) were also placed for comparison purposed when placed in the incubator. The cementation solutions (45 mL) were poured into

separate clean Falcon tubes (50 mL capacity) before being inoculated with overnight grown ureolytic bacterial cultures (5 mL). The mass of the dried precipitates was quantified. The deposits were placed in a centrifugation chamber (Eppendorf, 5804R, Germany) at 10,000g for 5 min. The obtained promises were placed on Whatman® filter paper (grade 1) in a constant drying oven-dried at 60 ˚C for 24 h. The weight (mass) of $CaCO_3$ precipitates was determined from measurements samples weighed before and after oven-drying. In addition, the effluents obtained after the biomineralization test were transferred into sterile beakers (100 mL), and their respective pH values were computed to account for the urease activity.

2.6. *Soil biocementation test*

The sandy soil used in this study for the biocementation improvement test was collected from Batu Kawah Sand Quarry (Phua Kheng Heng Sdn. Bhd.). A summary of the soil particle size distribution and some physicochemical characteristics is presented in **Table 3**. According to the Unified Soil Classification System (USCS), the soil was classified as a poorly graded sand (SP) [35]. Petri dishes were used in this experiment to serve as sand columns. The bottoms were perforated (4 holes having diameters of approximately 1.1 mm at the edge of the Petri dishes) with a syringe needle (19G) for drainage purposes (of the effluent). However, non-woven fabric was placed above the holes to avoid sand field leakage [14]. The influence of exogenous ureolytic bacterial cultures grown in POM mediums (GM-1 to GM-4) on MICP treatment for soil solidification was evaluated. Firstly, sand samples were autoclaved and dried in the oven before 50 g (of sands) were placed onto empty Petri dishes. 10 mL of cementation solution constituting equimolar (1M) of $CaCl_2$, and urea were carefully percolated into the columns. After 3 h, 20 mL of overnight grown bacterial cultures were added to the columns. The surficial treatment of the sand specimens was performed using Falcon tubes (50 mL capacity). The inflow rate of the treatment solution into the column was 25 mL/min. This biocementation treatment process was repeated two more days with two cycles per day. It is noteworthy that the new solutions and cultures were percolated at every cycle, and the wastewater (effluent) was discarded. The columns were then allowed to stay for curing (14 days) at room temperature (26 ˚C) before drying using an oven. Then, after treatment, the biocemented samples were collected for microstructural and mineralogical analyses.

2.7. *Scanning Electron Microscopy and Energy Dispersive X-ray Spectroscopy*

The scanning electron microscopy (SEM) and energy-dispersive X-ray spectroscopy (EDS) was performed following ASTM D8332 [36] and ASTM E1508-12a [37] standard procedures respectively. A Hitachi tabletop

microscope (TM4000, Hitachi, Ltd, Japan) with an accelerating voltage of 15 kV was used to examine the morphological structures and elemental composition of bio-treated soil particles containing crystal precipitates ureolytic bacterial activities. SEM pictograms of the sample surface morphologies were captured at magnifications of 250x and 10analysee EDS detector system by Bruker (Quantax 75) attached to the Hitachi benchtop microscope was used to scan, identify, and analyze the elemental composition percentages of the biocemented soil samples. The scanning is repeated numerous times at different surface areas of the soil samples until the preferred mineralogical results are selected and recorded [38].

2.8. *Fourier-transform infrared spectroscopy*

Fourier-transform infrared spectroscopy was performed to determine the *functional groups* and chemical bonds caused due to the MICP treatment on the biocemented soil specimens. A Fourier Transform Infrared Spectrophotometer (Shimadzu IRAffinity^{-1} machine, Japan) was used to scan the sample spectra resolution of 1 cm^{-1}. An estimated 0.5 mg specimens were mixed with 100 mg of dried spectroscopic grade potassium bromide powder in a clean agate pestle [39,40]. The samples were pelletised through vacuum pressure, being subjected to FTIR spectroscopy. Wavelengths ranging from 4000 to 400 cm^{-1} at 27 °C with 20 repeated scans were conducted according to ASTM E168-16 [41] and ASTM E1252-98 [42] standards for qualitative and quantitative analyses, respectively.

2.9. *Thermogravimetric analysis*

Thermogravimetric analysis (TGA) was used to measure the thermal stability and percentage weight (mass) loss of biocemented soil samples, either as a function of time or a function of temperature. The TGA analysis was performed using a TGA machine (Perkin Elmer, United States). An estimate of 20 mg of each sample was subjected to varying temperatures (40 to 500 °C) at a heating rate of 10 °C/min and a nitrogen flow rate of 20 mL/min. The TGA test was performed according to ASTM E168-10 [43], and ASTM E1131-08 [44] standards, respectively.

2.10. *Differential scanning calorimetry*

Differential scanning calorimetry (DSC) was performed to determine the type of response the biocemented sand specimens gave through heating. A DSC machine (Perkin Elmer, United States) was used to conduct the DSC analysis. The DSC test can study the melting point of crystalline polymer or glass transition point of material

following ASTM D3418-21 [45] and ASTM E1269-11(2018) [46] standards, respectively. An estimate of 5 mg of each biocemented sand specimen was sealed in an aluminium pan and subjected to heating that ranged from 40 to 400 °C at a heating rate of 10 °C/min [47].

2.11. Statistical analysis

All the experiments were carried out in triplicates, and the average mean results were attained. Microsoft Excel ® for Mac (version 16.62) was used to analyse and generate the result/figures in this study.

3. Results and discussion

3.1. Bacterial growth performance

The growth and pH curves of *S. pasteurii* are shown in **Fig. 3A** and **Fig. 3B**. The POM with different concentrations of yeast exact was applied as an alternative to conventional media for carbon and nutrient sources. The growth and pH data were continuously recorded for 24 h at an interval of 3 h. The OD represents the biomass concentration of the cultured bacterial cells [48]. On the other hand, changes in pH levels during the growth of ureolytic bacteria indicate urease activity and ammonium production. The growth curve of *S. pasteurii* in different cultivation mediums (GW-1 to GW-4) showed a steady increment throughout the incubation period. The initial OD_{600} ranged from 0.03 to 0.08. The elevation in the OD_{600} demonstrated that the *S. pasteurii* was growing steadily and acclimatizing to its new environments that were enriched with POM medium. The growth medium (GM-3 and GM-4) with lower yeast extract concentrations (4 g/L and 2 g/L) resulted in the lowest biomass concentration. **Fig. 3A** showed that the supplemented yeast extract in the medium did influence the biomass concentration. This meant that nutrients available in POM could support ureolytic bacterial growth but at a much slower rate when supplemented with low yeast extract. At the end of incubation (24 h), GM-1 and GM-2, which were supplemented with 8 g/L and 6 g/L yeast extract, had higher biomass concentrations (OD_{600} of 0.86 and 0.78, respectively) when compared with GM-3 (OD_{600} of 0.56) and GM-4 (OD_{600} of 0.48). The growth curves of the samples indicated that bacterial cells experienced growth lag and exponential phases. The bacterial cells seem to have taken a more extended period (15 h) to reach the exponential phase in GM-4.

In contrast, others had a relatively quicker lag phase before the exponential phase. *S. pasteurii* adapts to its high-nutrient microenvironment and strives for rapid development. During the exponential phase, cell growth accelerates, and nutrient consumption accelerates [14]. It also appeared that the trace metal elements present in

POM did not hinder bacterial growth. Nonetheless, to achieve high biomass concentration, the addition of supplementary nutrients should be considered. This is because nutrients such as yeast extract contain necessary vitamins and amino acids that can accelerate the development of bacterial cells [14].

The OD_{600} and pH profiles followed a similar pattern. The initial pH values at 0 h ranged from 6.96 to 7.13 for all the mediums. The increase in pH during bacterial cultivation is influenced by urease activity. Rising biomass concentration and medium pH of the microbial growth are regarded as suitable measures of the MICP operation [1]. The result in **Fig. 3B** showed that at the end of the incubation period, the pH levels for all mediums reached 9.07 to 9.24. This is regarded as the optimum pH condition of *S. pasteurii*. It is widely accepted that pH levels of the ureolytic bacteria reflect the MICP metabolism required for the $CaCO_3$ precipitation [16]. As the biomass increased, the pH levels of all mediums rapidly increased. Also, the growth trend of the pH values was almost the same for all samples as experienced in other studies [14,49]. Ureolytic bacteria are used in MICP and prefer alkaline conditions for their growth condition [48]. The increase of pH in the medium during bacterial cultivation is associated with the release of ammonium ions in the solution. Low pH induces $CaCO_3$ ion dissolution and lowers precipitation, whereas high pH enhances Ca immobilisation and electrochemical attraction [48].

Yeast extract is a protein-rich complex media that is conveniently used for bacterial cultivation. For MICP-related studies, 20 g/L of laboratory-grade yeast extract is often used to cultivate *S. pasteurii* [7,8,14,21,23,50–52]. However, some studies reported using 5 to 15 g/L of yeast extract [53–56]. Low-cost yeast extract was previously reported by to minimize bacterial growth for MICP up to 98% when compared with some conventional media (i.e., tryptic soy broth, cooked meat medium, nutrient broth, etc.) [56] However, a high amount of yeast extract was needed. It was recently suggested that supplementing cultivation media with waste material that contains essential components can positively impact the cultivation performance of the *S. pasteurii* [7]. In our preliminary study, we investigated the effect of POM without low-cost yeast extract on bacterial growth. It was found that after incubation for 48 h, the absorbance reading (OD_{600}), pH value, and urease activity were 0.39, 8.94 and2.44 mM urea hydrolysed/min.

The urease activities of *S. pasteurii* in the POM medium were evaluated end of the incubation period as shown in **Fig. 4**. The highest urease activity was 13.81 mM urea hydrolysed/min for GM1, while the lowest urease activity was 5.26 mM urea hydrolysed/min for GM 4. The urease activities of *S. pasteurii* in other mediums (GM 2 and GM 2) were 11.63 mM urea hydrolysed/min and 5.26 mM urea hydrolysed/min, respectively. The urease activities in GM 1 and GM 2 are comparable with our previous studies that reported the prospect of using food-

grade yeast extract for the ureolytic bacterial cultivation [9,57]. Higher ammonium ion concentration implies a higher urease activity rate due to a strong degree of ureolysis (urea hydrolysis). Also, an increase in the bacterial cell population can result in more production of urease enzyme [16].

3.2. Effect of varied concentrations of treatment solutions and temperatures on MICP

The effect of treatment solutions with various concentrations (0.25 M to 1.5 M, w/v) on MICP was studied. The cementation chemical is an essential component for promoting calcite precipitation. As a result, it is critical to provide adequate urea and calcium chloride to the soil [58]. Urea is a substrate that stimulates urease enzyme for carbonate production, and the presence of a calcium ion provides the necessary condition that permits $CaCO_3$ precipitation to occur [53]. During the biomineralisation test in the Falcon tubes, the instance bacterial cultures were inoculated, and visible cloudy precipitation formed. Irrespective of the cementation concentrations, the mixture with bacterial culture resulted in instant precipitation. After incubation, crystal precipitations or flocculation appeared at the bottom of the Falcon tubes. Lai et al. [51] also reported that higher cementation concentrations had more intense turbidity in their tests and higher $CaCO_3$ contents.

The $CaCO_3$ contents in **Fig. 5A** showed that at different concentrations of the cementation solution, the $CaCO_3$ contents differ. Equal molarities of urea and $CaCl_2$ at different concentrations were used for the biomineralisation test. This was to test the influence of the bacterial cultures grown on other cheap mediums to precipitate $CaCO_3$ minerals. As expected, ureolytic bacteria produced high biomass and used for the specimen (sample 1) had the highest $CaCO_3$ contents (0.84 g/mL to 4.59 g/mL). In comparison, sample 4 from bacteria grown in GM-4 produced the lowest $CaCO_3$ contents (0.34 g/mL to 1.58 g/mL). Based on this finding, to induce sufficient $CaCO_3$ crystals, ureolytic bacteria can be grown in an inexpensive, organic manure medium containing yeast-containing extract ranging from 4 g/L to 8 g/L.

Furthermore, the experiment's outcome demonstrated that the bacterial cultures exhibited tolerance to a high concentration of urea-$CaCl_2$, with a good crystal formation tendency [53]. A greater chemical concentration of treatment solution/mixture is required to precipitate more calcium carbonate in each treatment. However, with an increase in the concentration of treatment ingredients, the MICP process may be slowed or even terminated [51].

The purpose of testing the effect of different cementation concentrations on bacterial performance is because it can impact the strength of biocemented soil. Suitable urea-$CaCl_2$ concentration will produce denser crystal and biocemented soil with enhanced engineering properties. Hence, it is crucial to quantify the $CaCO_3$

precipitates and determine the cementation concentrations to better MICP efficiency. Furthermore, the effluent pH was studied from the supernatant in the Falcon tubes, as shown in **Fig. 5B**. The initial pH value of the treatment solution varied from pH 4 to 5, which indicated that these solutions were acidic. **Fig. 5B** suggested that the effluent pH attained steady neutrality to alkalinity. Although the pH values ranged from 6.27 to 7.56 for sample 1, pH 6.55 to 8.97 for sample 2, pH 6.87 to 8.59, and finally, pH 6.79 to 8.18 for sample 4.

The effluent pH solution transcended from alkaline to neutral or slightly acidic as the cementation concentration increased (from 0.25 M to 1.5 M). The observed pH variation in the effluent resolutions demonstrates the hydrolysis effect or ureolytic microbial capacity [59]. High pH values represent lost/unused urease activity in the effluent solution from the bacterial activity [3]. It is expected that different concentration levels of urea-$CaCl_2$ and urea hydrolysis will be affected. When effluent pH is high (especially at low cementation concentration), this solution should be recycled/reused during MICP treatment to improve microbial activity and biocementation. Finally, the results showed that the $CaCO_3$ content increased with the increasing concentration of cementation reagents for the MICP test. However, the results for effluent pH indicated that the pH level moved from alkaline to acidic with a growing concentration of cementation reagents.

Fig. 6A shows the effect of various temperatures on $CaCO_3$ content and the pH effluent after 48 h incubation. Temperature plays a vital role in the MICP process for bacterial biomass growth, urease production, and $CaCO_3$ formation [14]. Unsuitable temperature can influence carbonate precipitations by changing the bacterial urease activities [55]. This also happens to the solubility and chemical equilibrium of $CaCO_3$ precipitates during the MICP process. Hence, it is vital to test the effect of varying temperature conditions on precipitation rates of calcium carbonate. All the bacterial cultures grown in different mediums were able to induce carbonate crystals at temperatures that ranged from 10 ˚C to 50 ˚C. The results in **Fig. 6A** showed that at 10 ˚C, the lowest $CaCO_3$ contents were measured for all the tested samples except for sample 4. The highest $CaCO_3$ contents occurred when all the samples were incubated at 30ºC. For sample 4, the lowest $CaCO_3$ contents occurred at 50ºC. At different temperatures, the flocculants in the Falcon tubes increased with changes in incubation temperature. Interestingly, from sample 1 to sample 3, all the $CaCO_3$ contents increased until they reached 40ºC, where the measured precipitates decreased. It was also observed that the precipitation of carbonates (0.91 g/mL to 0.93 g/mL) for samples 1, 2, and 3 were comparable at 10ºC. This observation also occurred at 50ºC (1.76 g/mL to 1.74 g/mL) but only for samples 1 and 2.

Earlier research used *S. pasteurii* in MICP at low temperatures to show that the precipitation rate was too low to bind sand particles due to the low bacteria activity [55]. **Fig. 6A** demonstrated a correlation between

temperature and carbonate precipitation to a certain degree. Because the higher the temperature, the higher the precipitation rate during the incubation period except at 50ºC. This evidence suggests that it is preferable to use temperatures ranging from 20 ˚C to 40˚C for MICP when the bacterial is cultured in a cheap pelletised medium. It further confirms that *S. pasteurii* is sensitive to the changes in different temperature conditions for carbonate precipitation [55]. Recent studies demonstrated that these temperatures provided a suitable microenvironment to induce a high carbonate precipitates [20,48]. The authors suggested that very low temperatures (5 ˚C and below) and very high temperatures (5ºC and above) above the optimal threshold for MICP may deform the binding sites/surface activity and kinetic energy needed for soil biocementation. At extremely unfavourable conditions, the microbial cell structures would be inactivated owing to heat/cold, thus making it challenging for bacteria to execute regular metabolism for the urease production [20]. **Fig. 6B** indicated that the measured effluent pH values for the treated samples remained at a relatively neutral level. Irrespective of the temperature (10ºC to 50ºC) or bacterial cultures grown in different mediums (GM1 to GM4), the pH level did not drop to 6 or surpass 7.99. The highest effluent pH level at 10ºC and 20ºC occurred in sample 1. On the other hand, the highest effluent pH level at 40ºC and 50ºC was obtained from sample 2, while 30ºC was found in sample 3. However, the lowest effluent pH level in the tested samples at various temperatures occurred in sample 4.

3.3. *Analysis of crystal morphology and elemental composition*

The microstructural morphologies and mineralogical properties of crystals induced on the soil samples by the ureolytic bacterial cultures were determined using SEM-EDS analysis. **Fig. 7** presents the SEM images of the biocemented samples (four different treated specimens) after curing. The SEM images at 1000x magnification were able to visualize the presence of biomineral crystals on the specimens. Interestingly, soil sample-1 and sample-2 that were treated with ureolytic bacterial cultures grown with GM-1 and GM-2 had more crystal formations with lesser visible pore spaces in biocemented soil, as depicted in **Fig. 7A** and **Fig. 7B**. However, there were more visible voids with fewer crystal formations for samples treated with ureolytic bacterial cultures grown with GM-3 and GM-4. Soil voids become densely filled as the soil becomes subjected to MICP treatment due to the field's biocementation [60]. The soil pores in Fig. 9A and Fig. 9B appeared to have been filled with cementing material (i.e., $CaCO_3$) after the MICP treatment [8]. The SEM indicated that the precipitated crystals could change the morphological structures of soil particles by adhering to the surface of soil grains and bridging the particles together [21].

The crystal aggregates formed on the surface of soil particles or at the particle-to-particle interconnected pore spaces displayed irregular shapes with rough or smooth textures. Careful observation of SEM images for **Fig. 7A** and **Fig. 7B** suggested that these crystals showed clusters of rhombohedral shape. However, some biominerals appeared to be integrated into cubic-like forms with smooth surface textures. The significant difference between crystals displayed in these SEM images was the magnitude of their sizes when studied at higher magnification (1000x). The SEM analysis for **Fig. 7A** indicated that the crystals were more prominent in diameter (15 to 20 μm) when compared to **Fig. 7B,** which were slightly smaller in diameter (5 to 10 μm). Similar crystal morphological observations on MICP-treated soil samples were observed in previous studies [8,21,50,52]. Unfortunately, fewer crystals formed and adhered to the soil particles' surfaces for sample-3 and sample-4 after MICP treatment, as shown in **Fig. 7C** and **Fig. 7D**. It seemed the minerals were not properly crystallized when formed on the soil. More so, few noticeable crystals on these samples had cubic shapes. The SEM results showed that ureolytic bacteria grown in inexpensive POM (medium-1 and medium-2), which contained 60% (v/v) and 80% (v/v) of yeast extract, were able to induce more crystals during biocementation. Dissolved organic carbon release, protein, and other essential nutrients in cultivation media are crucial factors that can influence the formation/morphology of $CaCO_3$ crystals [4,9,10]. This is because the bacterial proliferation after cultivation provides the necessary condition (microbial activity) to induce the amount of $CaCO_3$ precipitate through the MICP process. This is evident in the result shown in **Fig. 7**. More treatment cycles (bacterial cultures and chemical solution) approach may be required during biocementation to achieve successful crystal shapes to bridge soil particles when using ureolytic bacteria grown in the inexpensive medium supplemented with low yeast extract.

The EDS analysis was performed after SEM to accurately determine the compositions of the microstructures (crystal minerals) formed after the soil MICP treatment test. The EDS spectra **(Fig. 8**) indicated the X-ray intensity emitted from each elemental composition. The brighter colour represents the more significant essential density/concentration [13,22,54] Clusters of biomineral crystals detected in the SEM micrographs confirm the presence of elements that correspond with carbonate minerals (i.e., $CaCO_3$). The EDS mapping was able to show the differences between the four treated soil samples based on mineralogical properties, as depicted in **Table 4**. For sample-1, the atom proportion for the leading elements was oxygen (32.6 %), carbon (25.3 %), and nitrogen (24.5 %). For sample-2, oxygen (60.5 %), carbon (16.3 %), and silicon (15.9 %) were the prominent elements. The major chemical elements identified by EDS analysis for sample-3 were oxygen (61.3 %), carbon (15.3 %), and silicon (12.2 %). Finally, the prominent elements for sample-2 were oxygen (44.7 %), carbon (20.5 %), and nitrogen (15.1 %). The overall atom percentage for soil sample-1 and sample-4 were oxygen, carbon, and nitrogen.

On the other hand, the dominant elements for soil sample-2 and sample-3 were oxygen, silicon, and carbon. In EDS mapping, the identified silicon element represents silicon dioxide, a constituent of sand [54,61].

The detection of carbon, oxygen, and calcium indicates the occurrence of biocementation, which can be used to bind soil particles. Bacterial cells produce negatively charged ions such as carbonate and hydroxide ions which provide conditions to bind with calcium ions and induce $CaCO_3$ precipitation. Theoretically, the formations of calcium carbonate mineral typically constitute carbon, oxygen, and calcium elements at an atomic ratio of 1:3:1 [62]. This relatively confirms the results presented in **Table 4** and **Fig. 8.** The main components of extracellular polymeric substances are polysaccharides, proteins, and nucleic acid, which are critical for biomineralisation during in MICP process [17]. Bacterial cells produce exopolysaccharides as a response to a toxic environment responsible for the biomineralisation of carbonate minerals [62]. The different atom proportions for the elements that constitute $CaCO_3$ may be influenced by this factor (extracellular polymeric substances). The detection of elements which includealuminiumm, calcium, iron, potassium, sodium, magnesium, and chlorine after EDS mapping may be related to the urea substrate and growth medium used for bacterial cultivation. It has been reported that these elements found in treated soil specimens are ascribed to organic matter secreted by bacteria cells [20]. It is also possible that they are attributed to the components of POM used in this study for bacterial cultivation. Like the SEM images, the EDS results showed that ureolytic bacterial cells cultivated in different constituents of growth medium have a profound effect on the elemental ratio compositions of $CaCO_3$ crystals.

3.4. *FTIR Spectroscopy*

The FTIR spectra for the biotreated specimens are shown in **Fig. 9**. The evaluated frequency vibrations were in the mid-infrared (400 to 4000 cm^{-1}) and near-infrared (4000 to 13000 cm^{-1}) regions [63] The bands in the region of 449.41 cm^{-1} (soil sample 2) and 466.77 cm^{-1} (soil sample 4) were attributed to weak C-C bending vibrations (out of the spectral window) [64]. The band presented at 536.21 cm^{-1} and 673.16 cm^{-1} detected in **Fig. 9D** were with medium C-I stretching vibration of aliphatic iodo compounds and medium C-H stretching vibration of alkyne group, respectively. A strong C-Cl stretching of aliphatic bromo compounds at wavelengths ranging from 769.60 cm^{-1} to 773.46 cm^{-1} was identified in all four MICP-treated soil samples.

These specified chemical bonds may be associated with the elements present in the organic waste material used in cultivating bacteria. The FTIR result showed strong, broad CO-O-CO stretching of anhydride (detected only in soil sample 4) and C-O stretching of primary alcohol (soil sample 3) at 1045.42 cm^{-1} and 1049.28 cm^{-1}, respectively. Strong S=O stretching vibration (1056.99 cm^{-1} to 1072.42 cm^{-1}) of sulfoxide and medium C-H in-plane bending vibration (1414.82 cm^{-1} to 1415.42 cm^{-1}) of vinyl were spotted except for **Fig. 9B**. A medium O-H

bending vibration of carboxylic acid at a wavelength of 1427.32 cm^{-1} was found only in sample 2. The C=C bending vibration of α, β-unsaturated ketone group occurred in **Fig. 9A** and **Fig. 9B**, at 1627.92 cm^{-1} and 1620.21 cm^{-1}, respectively. However, The C=C stretching vibration (1651.07 cm^{-1}) of vinylidene and the C=O stretching vibration (1791.87 cm^{-1}) of conjugated acid halide were only detected in **Fig. 9D**. Except for Fig. 8C, the FTIR results had C-H bending vibration of aromatic compound (overtone) at wavelengths ranging between 1809.23 cm^{-1} to 1878.67 cm^{-1}. Strong C=C=C stretching vibration of allene (1986.68 cm^{-1} to 1980.89 cm^{-1}) and weak CΞN stretching of nitrile (2237.43 cm^{-1} to 2245.14 cm^{-1}) were detected in all four soil samples. This vibration indicated that denitrification occurred during the MICP crystallisation process of the soil. Strong O=C=O stretching vibration of carbon dioxide at wavelengths ranging from 2370.51 cm^{-1} to 2385.95 cm^{-1} was shown in the FTIR results, except for **Fig. 9C**. The vibration peaks could be associated with carbonate precipitations since increased oxygen-containing surface functional group (i.e., carbonyl) enhances the crystal formation [65]. A medium C-H stretching vibration of the alkyne (2515.18 cm^{-1}) was found in **Fig. 9D**. The FTIR results in **Fig. 9A-C** further presented weak S-H stretching vibration of thiol at wavelengths between 2538.32 cm^{-1} to 2534.46 cm^{-1}. This may have occurred due to relevant biological materials such as proteins and enzymes associated with the reactive thiol group [66]. Medium C-H stretching vibration of alkene at wavelengths of 3170.97 cm^{-1} and 3153.61 cm^{-1} were shown in **Fig. 9B** and **Fig. 9C**, respectively. Previous research has revealed that these chemical bonding are useful for crystal aggregation and adherence of microorganisms [15,67]. A weak broad O-H stretching vibration of alcohol (intramolecular bonded) at wavelengths of 3284.77 cm^{-1} and 3250.05 cm^{-1} were detected in **Fig. 9B** and **Fig. 9D**, respectively. All the samples observed medium N-H stretching vibration (3354.21 cm^{-1} to 3417.86 cm^{-1}) of the aliphatic primary amine group and medium sharp O-H stretching vibration (3468.01 cm^{-1} to 3959.86 cm^{-1}) of the free hydroxyl group. These ascriptions of function groups generated due to MICP are suggested to belong to the stretching vibration of the organic matter [68]. The vibration of the hydroxyl group that was identified via FTIR verified the presence of water in the treated soil samples.

3.5. *TGA and DSC analyses of the biocemented specimens*

The TGA and DSC thermograph of the bio-treated soil particles after MICP treatment are shown in **Fig. 10** and **Fig. 11**. The figures indicate the GM-1 for soil sample-1, GM-2 for soil sample-2, GM-3 for soil sample-3, and GM-4 for soil sample-4. **Fig. 10** shows that soil sample-1, soil sample-2, soil sample-3, and soil sample-4 have a 3-step stoichiometric degradation process. The first degradation step was due to the loss of water in the crystallisation [69], which caused the deformation of the crystalline structure. For soil sample-1, the process

happened at early as 60°C and 150°C, while soil sample-2, soil sample-3, and soil sample-4 happened at 150 °C. At this stage, the soil sample loses volatile components such as moisture, solvents, and monomer. The second degradation step is due to the decomposition of the formation of calcium carbonate and the release of carbon monoxide for all samples. It is noted that all samples had a decomposition that started around 150°C to 200°C. The atmospheric switch from nitrogen to oxygen happened for soil sample-1 at 200°C to 280°C, but not for soil sample 2, soil sample -3, and soil sample-4. The third decomposition occurred at 250°C to 700°C for soil sample 2, soil sample 3, and soil sample 4. While for soil sample 1, it happened at 300°C to till 800°C. Around 700°C and above, combustion of carbon and the inert inorganic residue was notified for soil sample-2, soil sample-3, and soil sample 4. The degradation process for soil sample-1 is faster than for soil sample-2, soil sample-3, and soil sample-4. **Fig. 11** shows that almost all the soil samples had a similar reaction. The exothermic glass transition happened at 50°C, whereas glass formation happened slowly toward the first endothermic curve [70] from 180°C to 250°C. The endothermic curve was due to the melting process of the partially crystalline soil sample due to the heat [32].

3.6. *Cost implication*

The typical materials required for MICP include nutrient source, urea, and calcium chloride. Most (60%) of these material expenses are spent on bio-stimulation of native/indigenous ureolytic microorganisms or bio-augmentation of exogenous ureolytic microorganisms [33]. Omoregie et al. [56] previously showed that the food-grade Yeast extract (Angel Yeast/FB00) cost US$ 0.27 for 15 g/L which was 89.89% cheaper than laboratory-grade yeast extract (BD BACTO™/ #212750). However, this present study showed that POM has the potential for circular economy and is useful for MICP application. The addition of 2 to 8g/L of cheap yeast extract in the POM medium results in a total culture cost of US$ 0.32 to US$ 0.41, considering if the POM is procured from a supplier. This further indicates that using POM has the potential to serve as an alternative medium to the present cultivation medium. Also, the scholarly community will benefit from cost savings, and the introduction of less hazardous materials into the geoenvironment, if POM is used for bacterial cultivation. Kitchen waste was recently used to grow *S. pasteurii* for wind erosion control of arid soil [14]. The authors demonstrated that kitchen waste (0.375 g/L) was less expensive (less than US$ 1) than traditional media (yeast extract medium, nutritional broth medium, and tryptic soy broth medium, 1 to US$ 5, respectively). Another study showed that MICP cultivation cost was reduced from US$ 2.34/L (Laboratory-grade reagents) to US$ 0.28/L (low-grade reagents) for field-scale application [71]. This means that future researchers should aim to reduce the cost of bacterial cultivation to $1 or less, and it is suggested that cheaper materials be used for MICP studies and applications.

The material cost of MICP is also determined by the cost of chemical reagents such as calcium chloride, and urea. For cost reduction of these chemicals, researchers have proposed other alternatives. A recent study demonstrated that thermally treated cow urine is a viable alternative to synthetic urea for MICP application. The authors showed that this cow urine maintained the desired pH range (7 to 9) for over 28 days of monitoring without requiring an additional item for the stability [72]. Another recent paper demonstrated that fresh urine and carbide sludge (containing 30% of Calcium hydroxide, w/w) can help significantly lower the expense of urea and calcium supply for MICP applications [73]. The urine was filtered using a filter paper (pore size of 6 µm) and sterilized via ultraviolet for 6 h before use. The authors reported that after treating their sand, they obtained uniaxial compressive strength, calcium carbonate content, and permeability values of 1.7 MPa, 7.7%, and 4.1×10^{-6} m/s, respectively [73]. Another recent work showed that eggshell waste material can serve as a suitable alternative to calcium source since it contains 94% of calcium salts [74]. To further reduce MICP chemical reagents, future studies can explore using fish bones, chicken bones, and seafood shells (i.e., clam shells, and blood cockle shells). These can be explored as alternative replacements to calcium chloride. In addition, Waste from a horse shelter can be used to replace urea instead of fertilizer or technical-grade urea.

4. Conclusion

It is concluded that low-cost POM, containing yeast extract ranging from 4 g/L to 8 g/L can serve as an alternative bacterial cultivation nutrient source for the MICP process. POM supplemented with more yeast extract inclusion had higher biomass concentrations, demonstrating that the combination of low-grade/food-grade yeast extract and POM can lower bacterial cultivation costs. The pH levels for all mediums reached 9.07 to 9.24, which is regarded as the optimum pH condition of *Sporosarcina pasteurii* and the pH level moved from alkaline to acidic with increasing concentration of cementation reagents. It is preferable to use temperatures ranging from 20°C to 40°C for MICP when the bacterial is cultured in the low-cost POM medium. Further analyses (SEM-EDX, FTIR, TGA, and DSC) on the biocemented soil specimens showed that the compositions of nutrients used in growing ureolytic bacterial cells have a profound effect on the crystal formation during MICP. The vibration indicated in the FTIR spectra for biotreated soil specimen confirms that denitrification occurred during the MICP crystallization process of the soil. The TGA and DSC thermograph of the bio-treated soil particles indicated degradation due to the loss of water in crystallization and the decomposition of calcium carbonate with the release of carbon monoxide. POM combined with low-grade/food-grade yeast extract is recommended as a low-cost alternative nutrient source in the cultivation of the *Sporosarcina pasteurii* strain for a more economically sustainable and eco-friendly MICP biocementation application.

Ethical Approval

Not applicable.

Competing interests

The authors declare no competing interests.

Authors' contributions

The first manuscript draft and part of the experiments were performed by A.I. Omoregie. Project supervision and administrative work were performed by K. Muda. Some of the experimental analyses (i.e., SEM-EDS, FTIR, TGA, and DSC) were conducted by M.K.B. Bakri, M.R. Rahman, and F.A.M. Yusof. The manuscript was critically reviewed and edited by O.O. Ojuri. All authors read and approved the final manuscript before submission.

Funding

This study was funded by the Universiti Teknologi Malaysia (Grant No. 05E84).

Availability of data and materials

The datasets generated and/or evaluated during the present research are available upon reasonable request from the corresponding author.

References

[1] Y. Al-Salloum, S. Hadi, H. Abbas, T. Almusallam, M.A. Moslem, Bio-induction and bioremediation of cementitious composites using microbial mineral precipitation – A review, Constr. Build. Mater. 154 (2017) 857–876. https://doi.org/10.1016/j.conbuildmat.2017.07.203.

[2] T. Wei, H. Li, N. Yashir, X. Li, H. Jia, X. Ren, J. Yang, L. Hua, Effects of urease-producing bacteria and eggshell on physiological characteristics and Cd accumulation of pakchoi (Brassica chinensis L.) plants, Environ. Sci. Pollut. Res. 29 (2022) 2924–2935. https://doi.org/10.1007/s11356-022-20344-5.

[3] L. Cheng, R. Cord-Ruwisch, In situ soil cementation with ureolytic bacteria by surface percolation, Ecol. Eng. 42 (2012) 64–72. https://doi.org/10.1016/j.ecoleng.2012.01.013.

[4] N.K. Dhami, A. Mukherjee, M.S. Reddy, Micrographical, minerological and nano-mechanical characterisation of microbial carbonates from urease and carbonic anhydrase producing bacteria, Ecol. Eng. (2016). https://doi.org/10.1016/j.ecoleng.2016.06.013.

[5] X. Deng, Z. Yuan, Y. Li, H. Liu, J. Feng, B. de Wit, Experimental study on the mechanical properties of microbial mixed backfill, Constr. Build. Mater. 265 (2020). https://doi.org/10.1016/j.conbuildmat.2020.120643.

[6] J. Xiang, J. Qiu, Y. Wang, X. Gu, Calcium acetate as calcium source used to biocement for improving performance and reducing ammonia emission, J. Clean. Prod. 348 (2022) 131286. https://doi.org/https://doi.org/10.1016/j.jclepro.2022.131286.

[7] F.M. Lapierre, J. Schmid, B. Ederer, N. Ihling, J. Büchs, R. Huber, Revealing nutritional requirements of MICP-relevant Sporosarcina pasteurii DSM33 for growth improvement in chemically defined and complex media, Sci. Rep. 10 (2020). https://doi.org/10.1038/s41598-020-79904-9.

[8] S.M. Ezzat, A.Y.I. Ewida, Smart soil grouting using innovative urease-producing bacteria and low cost materials, J. Appl. Microbiol. (2021). https://doi.org/10.1111/jam.15117.

[9] A.I. Omoregie, E.A. Palombo, D.E.L. Ong, P.M. Nissom, Biocementation of sand by Sporosarcina pasteurii strain and technical-grade cementation reagents through surface percolation treatment method, Constr. Build. Mater. 228 (2019). https://doi.org/10.1016/j.conbuildmat.2019.116828.

[10] S. Gowthaman, T.H.K. Nawarathna, P.G.N. Nayanthara, K. Nakashima, S. Kawasaki, The Amendments in Typical Microbial Induced Soil Stabilization by Low-Grade Chemicals, Biopolymers and Other Additives: A Review, in: V. Achal, C.S. Chin (Eds.), Build. Mater. Sustain. Ecol. Environ., Springer Singapore, Singapore, 2021: pp. 49–72. https://doi.org/10.1007/978-981-16-1706-5_4.

[11] M.G. Gomez, C.M. Anderson, C.M.R. Graddy, J.T. DeJong, D.C. Nelson, T.R. Ginn, Large-scale comparison of bioaugmentation and biostimulation approaches for biocementation of sands, J. Geotech. Geoenvironmental Eng. 143 (2017). https://doi.org/10.1061/(ASCE)GT.1943-5606.0001640.

[12] M. Al Imran, S. Gowthaman, K. Nakashima, S. Kawasaki, M. Al Imran, S. Gowthaman, K. Nakashima, S. Kawasaki, The Influence of the Addition of Plant-Based Natural Fibers (Jute) on Biocemented Sand Using MICP Method, Materials (Basel). 13 (2020) 4198. https://doi.org/10.3390/MA13184198.

[13] A.A. Dubey, K. Ravi, M.A. Shahin, N.K. Dhami, A. Mukherjee, Bio-composites treatment for mitigation of current-induced riverbank soil erosion, Sci. Total Environ. 800 (2021). https://doi.org/10.1016/j.scitotenv.2021.149513.

[14] H. Meng, S. Shu, Y. Gao, J. He, Y. Wan, Kitchen waste for Sporosarcina pasteurii cultivation and its application in wind erosion control of desert soil via microbially induced carbonate precipitation, Acta Geotech. (2021). https://doi.org/10.1007/s11440-021-01334-2.

[15] W. Yang, A. Ali, J. Su, J. Liu, Z. Wang, L. Zhang, Microbial induced calcium precipitation based anaerobic immobilized biofilm reactor for fluoride, calcium, and nitrate removal from groundwater, Chemosphere. 295 (2022) 133955. https://doi.org/https://doi.org/10.1016/j.chemosphere.2022.133955.

[16] Z.-F. Xue, W.-C. Cheng, L. Wang, W. Hu, Effects of bacterial inoculation and calcium source on microbial-induced carbonate precipitation for lead remediation, J. Hazard. Mater. 426 (2022) 128090. https://doi.org/https://doi.org/10.1016/j.jhazmat.2021.128090.

[17] S. Qiao, G. Zeng, X. Wang, C. Dai, M. Sheng, Q. Chen, F. Xu, H. Xu, Multiple heavy metals immobilization based on microbially induced carbonate precipitation by ureolytic bacteria and the precipitation patterns exploration, Chemosphere. 274 (2021). https://doi.org/10.1016/j.chemosphere.2021.129661.

[18] B. Kristiansen, Process economics, in: C. Ratledge, B. Kristiansen (Eds.), Basic Biotechnol., 3rd ed., Cambridge University Press, Cambridge, 2006: pp. 271–286. https://doi.org/10.1017/CBO9780511802409.013.

[19] A.I. Omoregie, L.H. Ngu, D.E.L. Ong, P.M. Nissom, Low-cost cultivation of Sporosarcina pasteurii strain in food-grade yeast extract medium for microbially induced carbonate precipitation (MICP) application, Biocatal. Agric. Biotechnol. 17 (2019) 247–255. https://doi.org/10.1016/j.bcab.2018.11.030.

[20] H. Yi, T. Zheng, Z. Jia, T. Su, C. Wang, Study on the influencing factors and mechanism of calcium carbonate precipitation induced by urease bacteria, J. Cryst. Growth. 564 (2021). https://doi.org/10.1016/j.jcrysgro.2021.126113.

[21] Y. Yang, J. Chu, B. Cao, H. Liu, L. Cheng, Biocementation of soil using non-sterile enriched urease-producing bacteria from activated sludge, J. Clean. Prod. 262 (2020) 121315. https://doi.org/https://doi.org/10.1016/j.jclepro.2020.121315.

[22] S. Lee, J. Kim, An Experimental Study on Enzymatic-Induced Carbonate Precipitation Using Yellow Soybeans for Soil Stabilization, KSCE J. Civ. Eng. 24 (2020) 2026–2037. https://doi.org/10.1007/s12205-020-1659-9.

[23] A. Amiri, Z.B. Bundur, Use of corn-steep liquor as an alternative carbon source for biomineralization in cement-based materials and its impact on performance, Constr. Build. Mater. 165 (2018) 655–662. https://doi.org/10.1016/j.conbuildmat.2018.01.070.

[24] Anu, A. Kumar, D. Singh, V. Kumar, B. Singh, Production of cellulolytic enzymes by Myceliophthora

thermophila and their applicability in saccharification of rice straw, Biomass Convers. Biorefinery. 12 (2022) 2649–2662. https://doi.org/10.1007/s13399-020-00783-1.

[25] D. Vidya, K. Nayana, M. Sreelakshmi, K. V Keerthi, K.S. Mohan, M.P. Sudhakar, K. Arunkumar, A sustainable cultivation of microalgae using dairy and fish wastes for enhanced biomass and bio-product production, Biomass Convers. Biorefinery. (2021). https://doi.org/10.1007/s13399-021-01817-y.

[26] M. Kimura, Testing methods for fertilizers, Japan, 2013. http://www.famic.go.jp/ffis/fert/obj/TestingMethodsForFertilizers2013.pdf.

[27] ASTM E1621-21, Standard Guide for Elemental Analysis by Wavelength Dispersive X-Ray Fluorescence Spectrometry, 2021. https://doi.org/10.1520/E1621-21.

[28] O.A. Cuzman, K. Richter, L. Wittig, P. Tiano, Alternative nutrient sources for biotechnological use of Sporosarcina pasteurii, World J. Microbiol. Biotechnol. 31 (2015) 897–906. https://doi.org/10.1007/s11274-015-1844-z.

[29] S.L. Williams, M.J. Kirisits, R.D. Ferron, Optimization of growth medium for Sporosarcina pasteurii in bio-based cement pastes to mitigate delay in hydration kinetics, J. Ind. Microbiol. Biotechnol. 43 (2016) 567–575. https://doi.org/10.1007/s10295-015-1726-2.

[30] J. Wu, X.-B. Wang, H.-F. Wang, R.J. Zeng, Microbially induced calcium carbonate precipitation driven by ureolysis to enhance oil recovery, RSC Adv. 7 (2017) 37382–37391. https://doi.org/10.1039/C7RA05748B.

[31] C.A. Spencer, L. van Paassen, H. Sass, Effect of jute fibres on the process of MICP and properties of biocemented sand, Materials (Basel). 13 (2020) 1–24. https://doi.org/10.3390/ma13235429.

[32] A. Clarà Saracho, S.K. Haigh, T. Hata, K. Soga, S. Farsang, S.A.T. Redfern, E. Marek, Characterisation of CaCO3 phases during strain-specific ureolytic precipitation, Sci. Rep. 10 (2020) 1–12. https://doi.org/10.1038/s41598-020-66831-y.

[33] V.V.S. Whiffin, Microbial CaCO3 Precipitation for the Production of Biocement, Phd Thesis. (2004) 1–162. https://doi.org/http://researchrepository.murdoch.edu.au/399/2/02Whole.pdf.

[34] M.P. Harkes, L.A. van Paassen, J.L. Booster, V.S. Whiffin, M.C.M. van Loosdrecht, Fixation and distribution of bacterial activity in sand to induce carbonate precipitation for ground reinforcement, Ecol. Eng. 36 (2010) 112–117. https://doi.org/10.1016/j.ecoleng.2009.01.004.

[35] ASTM, Standard Practice for Classification of Soils for Engineering Purposes (Unified Soil Classification System), ASTM International, 2020.

[36] ASTM D8332, Standard Practice for Collection of Water Samples with High, Medium, or Low Suspended Solids for Identification and Quantification of Microplastic Particles and Fibers, 2020.

[37] ASTM E1508-12a, Standard Guide for Quantitative Analysis by Energy-Dispersive Spectroscopy, 2019. https://doi.org/10.1520/E1508-12AR19.

[38] M.Y. Chin, M. Rahman, K.K. Kuok, W.Y. Chiew, M.K.B. Bakri, Characterization and Impact of Curing Duration on the Compressive Strength of Coconut Shell Coarse Aggregate in Concrete, BioResources. 16 (2021). https://doi.org/10.15376/biores.16.3.6057-6073.

[39] S. Fatma, A. Saleem, R. Tabassum, Wheat straw hydrolysis by using co-cultures of Trichoderma reesei and Monascus purpureus toward enhanced biodegradation of the lignocellulosic biomass in bioethanol biorefinery, Biomass Convers. Biorefinery. 11 (2021) 743–754. https://doi.org/10.1007/s13399-020-00652-x.

[40] M.J. Kamran, E. Jayamani, S.K. Heng, Y.C. Wong, M.R. Rahman, A.S. Al-Bogami, D. Huda, M.K. Bin Bakri, M.M. Rahman, Characterization and Comparative Study on Chemically Treated Luffa Fiber as Reinforcement for Polylactic Acid Bio-composites, BioResources. 17 (2022) 2576–2597. https://doi.org/10.15376/biores.17.2.2576-2597.

[41] ASTM E168-16, Standard Practices for General Techniques of Infrared Quantitative Analysis, 2016.

[42] ASTM E1252-98, Standard Practice for General Techniques for Obtaining Infrared Spectra for Qualitative Analysis, 2021. https://doi.org/10.1520/E1252-98R21.

[43] ASTM E1868-10, Standard Test Methods for Loss-On-Drying by Thermogravimetry, 2021.

[44] ASTM E1131-20, Standard Test Method for Compositional Analysis by Thermogravimetry, 2020.

[45] ASTM D3418-21, Standard Test Method for Transition Temperatures and Enthalpies of Fusion and Crystallization of Polymers by Differential Scanning Calorimetry, 2021. https://doi.org/https://www.astm.org/d3418-21.html.

[46] A. E1269-11(2018), Standard Test Method for Determining Specific Heat Capacity by Differential Scanning Calorimetry, 2018. https://doi.org/https://www.astm.org/e1269-11r18.html.

[47] P.L.N. Khui, M.R. Rahman, A.S. Ahmed, K.K. Kuok, M.K. Bin Bakri, D. Tazeddinova, Z.A. Kazhmukanbetkyzy, B.B. Torebek, Morphological and Thermal Properties of Composites Prepared with Poly (lactic acid), Poly (ethylene-alt-maleic anhydride), and Biochar from Microwave-pyrolyzed Jatropha Seeds, BioResources. 16 (2021) 3171–3185.

[48] A. Ali, M. Li, J. Su, Y. Li, Z. Wang, Y. Bai, E.F. Ali, S.M. Shaheen, Brevundimonas diminuta isolated

from mines polluted soil immobilized cadmium (Cd2+) and zinc (Zn2+) through calcium carbonate precipitation: Microscopic and spectroscopic investigations, Sci. Total Environ. 813 (2022) 152668. https://doi.org/https://doi.org/10.1016/j.scitotenv.2021.152668.

[49] L. Wang, S. Liu, Mechanism of sand cementation with an efficient method of microbial-induced calcite precipitation, Materials (Basel). 14 (2021). https://doi.org/10.3390/ma14195631.

[50] C.-M. Hsu, Y.-H. Huang, V.R. Nimje, W.-C. Lee, H.-J. Chen, Y.-H. Kuo, C.-H. Huang, C.-C. Chen, C.-Y. Chen, Comparative study on the sand bioconsolidation through calcium carbonate precipitation by sporosarcina pasteurii and bacillus subtilis, Crystals. 8 (2018). https://doi.org/10.3390/cryst8050189.

[51] H.-J. Lai, M.-J. Cui, S.-F. Wu, Y. Yang, J. Chu, Retarding effect of concentration of cementation solution on biocementation of soil, Acta Geotech. 16 (2021) 1457–1472. https://doi.org/10.1007/s11440-021-01149-1.

[52] X. Xu, H. Guo, X. Cheng, M. Li, The promotion of magnesium ions on aragonite precipitation in MICP process, Constr. Build. Mater. 263 (2020). https://doi.org/10.1016/j.conbuildmat.2020.120057.

[53] S. Zhu, X. Hu, Y. Zhao, Y. Fan, M. Wu, W. Cheng, P. Wang, S. Wang, Coal Dust Consolidation Using Calcium Carbonate Precipitation Induced by Treatment with Mixed Cultures of Urease-Producing Bacteria, Water. Air. Soil Pollut. 231 (2020). https://doi.org/10.1007/s11270-020-04815-4.

[54] X. Yu, H. Rong, Seawater based MICP cements two/one-phase cemented sand blocks, Appl. Ocean Res. 118 (2022) 102972. https://doi.org/https://doi.org/10.1016/j.apor.2021.102972.

[55] X. Sun, L. Miao, T. Tong, C. Wang, Study of the effect of temperature on microbially induced carbonate precipitation, Acta Geotech. 14 (2019) 627–638. https://doi.org/https://doi.org/10.1007/s11440-018-0758-y.

[56] A.I. Omoregie, D.E.L. Ong, P.M. Nissom, Assessing ureolytic bacteria with calcifying abilities isolated from limestone caves for biocalcification, Lett. Appl. Microbiol. 68 (2019) 173–181. https://doi.org/10.1111/lam.13103.

[57] A.I. Omoregie, E.A. Palombo, D.E.L. Ong, P.M. Nissom, A feasible scale-up production of Sporosarcina pasteurii using custom-built stirred tank reactor for in-situ soil biocementation, Biocatal. Agric. Biotechnol. 24 (2020) 101544. https://doi.org/10.1016/j.bcab.2020.101544.

[58] L.M. Lee, W.S. Ng, C.K. Tan, S.L. Hii, Bio-Mediated Soil Improvement under Various Concentrations of Cementation Reagent, Appl. Mech. Mater. 204–208 (2012) 326–329. https://doi.org/10.4028/www.scientific.net/AMM.204-208.326.

765 [59] M. Al Imran, S. Kimura, K. Nakashima, N. Evelpidou, S. Kawasaki, Feasibility study of native ureolytic
766 bacteria for biocementation towards coastal erosion protection by MICP method, Appl. Sci. 9 (2019).
767 https://doi.org/10.3390/app9204462.
768 [60] S. Mukherjee, R.B. Sahu, J. Mukherjee, Effect of Biologically Induced Cementation via Ureolysis in
769 Stabilization of Silty Soil, Geomicrobiol. J. 39 (2022) 66–82.
770 https://doi.org/10.1080/01490451.2021.2005188.
771 [61] S. Guo, J. Zhang, M. Li, N. Zhou, W. Song, Z. Wang, S. Qi, A preliminary study of solid-waste coal
772 gangue based biomineralization as eco-friendly underground backfill material: Material preparation and
773 macro-micro analyses, Sci. Total Environ. 770 (2021) 145241.
774 https://doi.org/https://doi.org/10.1016/j.scitotenv.2021.145241.
775 [62] S. Sepúlveda, C. Duarte-Nass, M. Rivas, L. Azócar, A. Ramírez, J. Toledo-Alarcón, L. Gutiérrez, D.
776 Jeison, Á. Torres-Aravena, Testing the capacity of staphylococcus equorum for calcium and copper
777 removal through MICP process, Minerals. 11 (2021). https://doi.org/10.3390/min11080905.
778 [63] A.B.D. Nandiyanto, R. Oktiani, R. Ragadhita, How to read and interpret FTIR spectroscope of organic
779 material, Indones. J. Sci. Technol. 4 (2019) 97–118. https://doi.org/10.17509/ijost.v4i1.15806.
780 [64] D.I. Santos, M.J. Neiva Correia, M.M. Mateus, J.A. Saraiva, A.A. Vicente, M. Moldão, Fourier
781 Transform Infrared (FT-IR) Spectroscopy as a Possible Rapid Tool to Evaluate Abiotic Stress Effects on
782 Pineapple By-Products, Appl. Sci. 9 (2019). https://doi.org/10.3390/app9194141.
783 [65] X. Chen, V. Achal, Biostimulation of carbonate precipitation process in soil for copper immobilization,
784 J. Hazard. Mater. 368 (2019) 705–713. https://doi.org/10.1016/j.jhazmat.2019.01.108.
785 [66] P. Bazylewski, R. Divigalpitiya, G. Fanchini, In situ Raman spectroscopy distinguishes between
786 reversible and irreversible thiol modifications in l-cysteine, RSC Adv. 7 (2017) 2964–2970.
787 https://doi.org/10.1039/C6RA25879D.
788 [67] L. Yang, L.-K. Guo, Y.-X. Ren, J.-W. Dou, P.-T. Zhu, S. Cui, Z.-H. Zhang, X.-T. Li, Denitrification
789 performance, biofilm formation and microbial diversity during startup of slow sand filter using powdery
790 polycaprolactone as solid carbon source, J. Environ. Chem. Eng. 9 (2021) 105561.
791 https://doi.org/https://doi.org/10.1016/j.jece.2021.105561.
792 [68] H. Rong, C.-X. Qian, Binding Functions of Microbe Cement, Adv. Eng. Mater. 17 (2015) 334–340.
793 https://doi.org/https://doi.org/10.1002/adem.201400030.
794 [69] E. Zhang, T. Wang, K. Yu, J. Liu, W. Chen, A. Li, H. Rong, R. Lin, S. Ji, X. Zheng, Y. Wang, L.

Zheng, C. Chen, D. Wang, J. Zhang, Y. Li, Bismuth Single Atoms Resulting from Transformation of Metal–Organic Frameworks and Their Use as Electrocatalysts for CO2 Reduction, J. Am. Chem. Soc. 141 (2019) 16569–16573. https://doi.org/10.1021/jacs.9b08259.

[70] B. Bafarawa, A. Nepryahin, L. Ji, E.M. Holt, J. Wang, S.P. Rigby, Combining mercury thermoporometry with integrated gas sorption and mercury porosimetry to improve accuracy of pore-size distributions for disordered solids, J. Colloid Interface Sci. 426 (2014) 72–79. https://doi.org/https://doi.org/10.1016/j.jcis.2014.03.053.

[71] A.B. Cunningham, A.J. Phillips, E. Troyer, E. Lauchnor, R. Hiebert, R. Gerlach, L. Spangler, Wellbore leakage mitigation using engineered biomineralization, Energy Procedia. 63 (2014) 4612–4619. https://doi.org/10.1016/j.egypro.2014.11.494.

[72] C. Comadran-Casas, C.J. Schaschke, J.C. Akunna, M.E. Jorat, Cow urine as a source of nutrients for Microbial-Induced Calcite Precipitation in sandy soil, J. Environ. Manage. 304 (2022) 114307. https://doi.org/https://doi.org/10.1016/j.jenvman.2021.114307.

[73] Y. Yang, J. Chu, L. Cheng, H. Liu, Utilization of carbide sludge and urine for sustainable biocement production, J. Environ. Chem. Eng. 10 (2022) 107443. https://doi.org/https://doi.org/10.1016/j.jece.2022.107443.

[74] P. Kulanthaivel, B. Soundara, S. Selvakumar, A. Das, Application of waste eggshell as a source of calcium in bacterial bio-cementation to enhance the engineering characteristics of sand, Environ. Sci. Pollut. Res. (2022). https://doi.org/10.1007/s11356-022-20484-8.

Acknowledgements

A.I. Omoregie appreciates the financial support received from Universiti Teknologi Malaysia in form of research grants (Grant No. 05E84). The authors would also like to thank Universiti Malaysia Sarawak and Universiti Kuala Lumpur for their providing equipment used for SEM-EDS, FTIR, DSC and TGA analyses.

List of figures

Fig. 1: Packets of POM purchased to serve as an inexpensive alternative cultivation medium.

Fig. 2: Images showing shake flasks containing POM medium (A) before and (B) after cultivation of *S. pasteurii*.

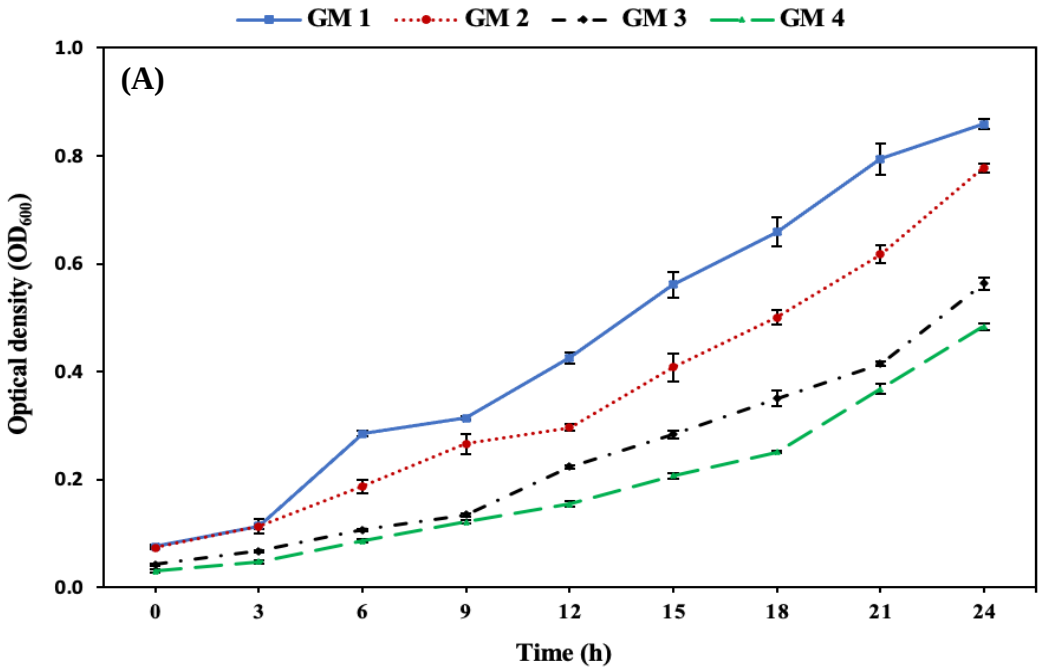

838

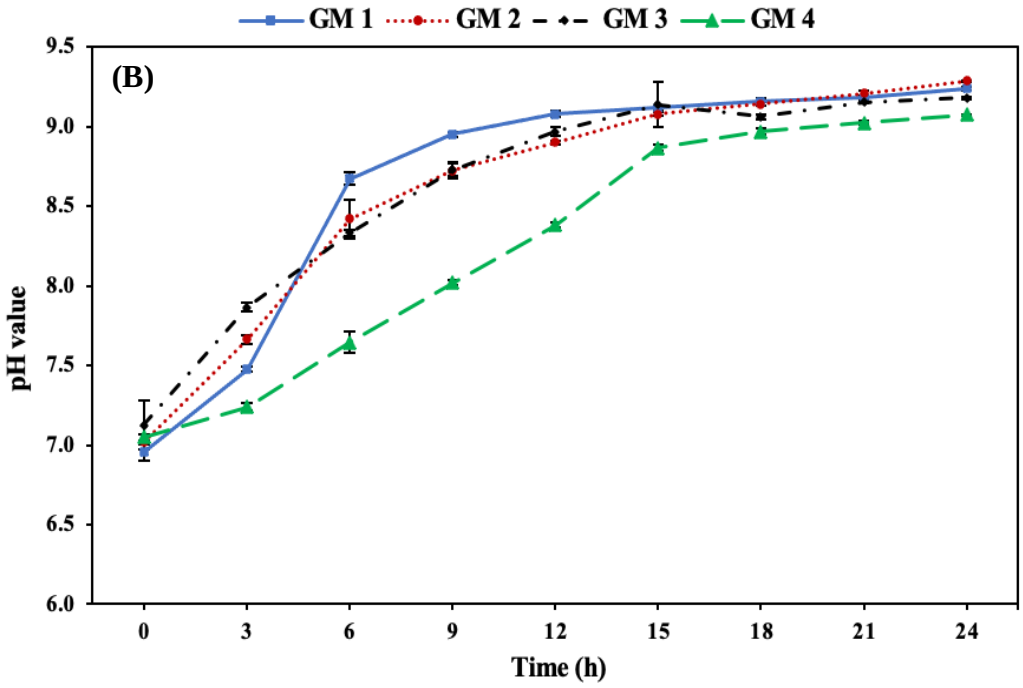

839

840 **Fig. 3:** Growth and pH profiles of *S. pasteurii* in POM medium containing various concentrations of low-grade

841 yeast extract (2 g/L to 8 g/L). Error bars represent standard deviations.

842

843

844

845

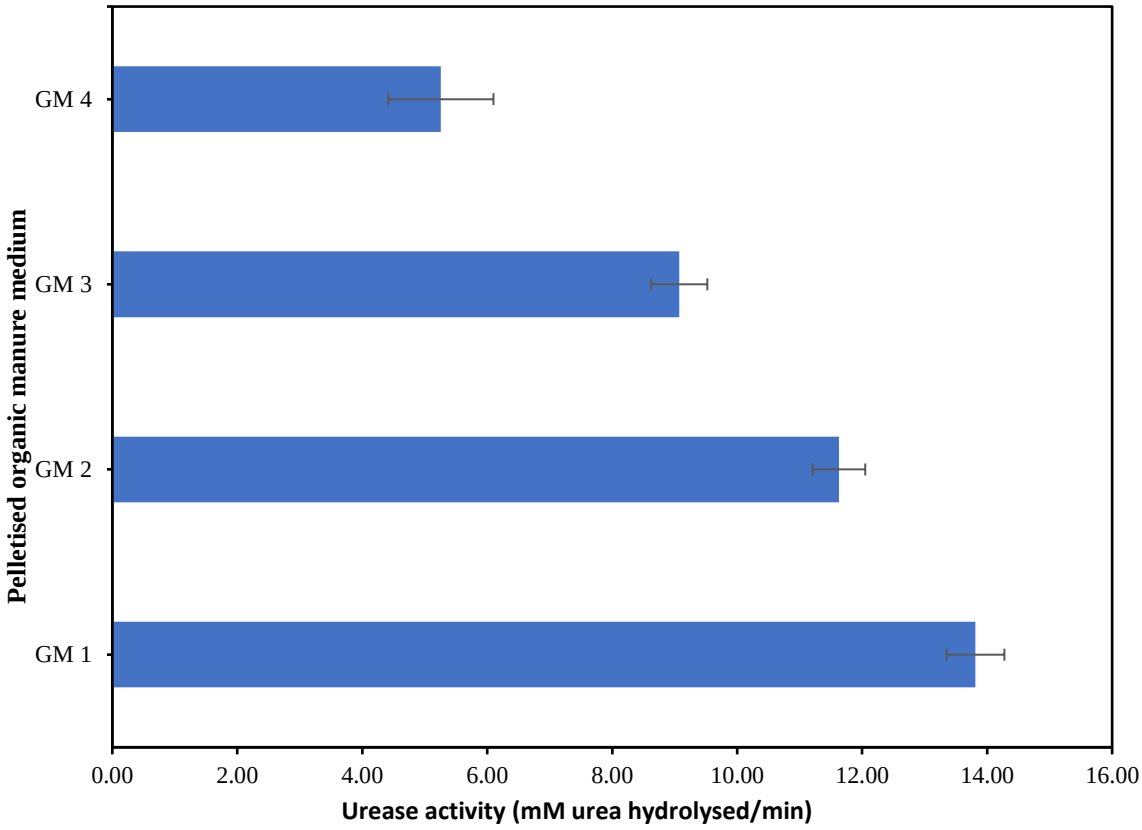

Fig. 4: Urease activity of *S. pasteurii* after cultivation in POM medium.

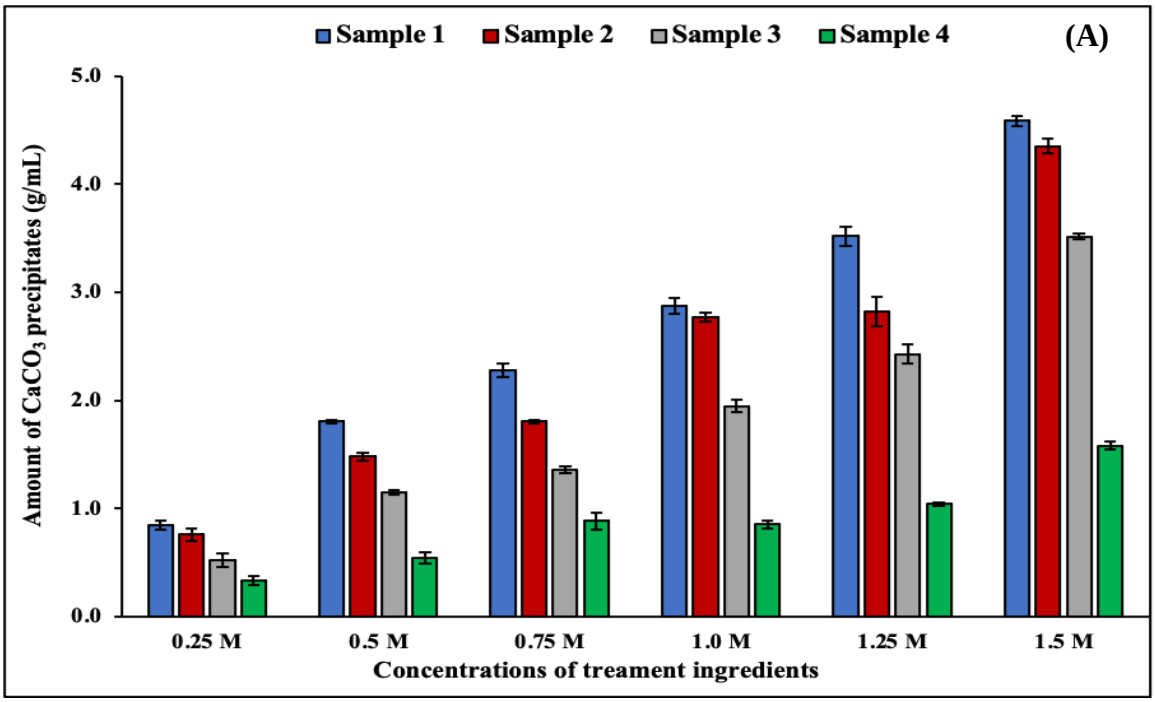

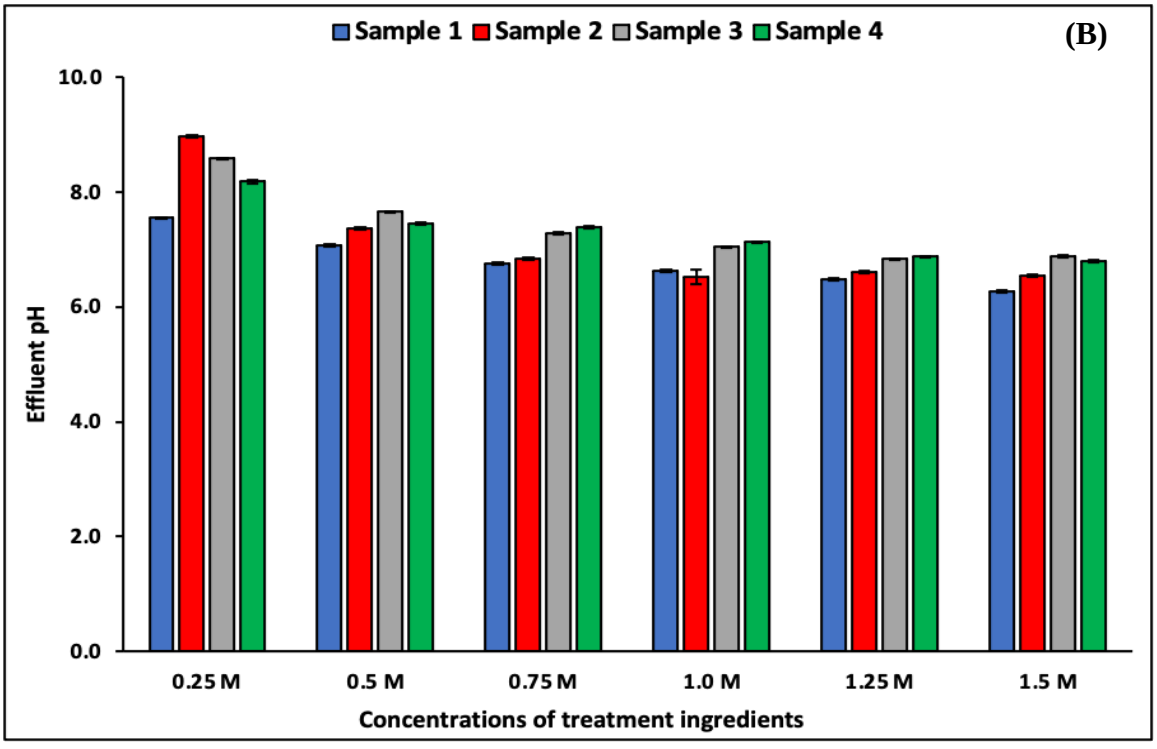

Fig. 5: Effect of various concentrations of treatment solution on treated specimens. (A) Mass of $CaCO_3$ contents, and (B) pH of the effluent solutions. The error bars represent standard deviations.

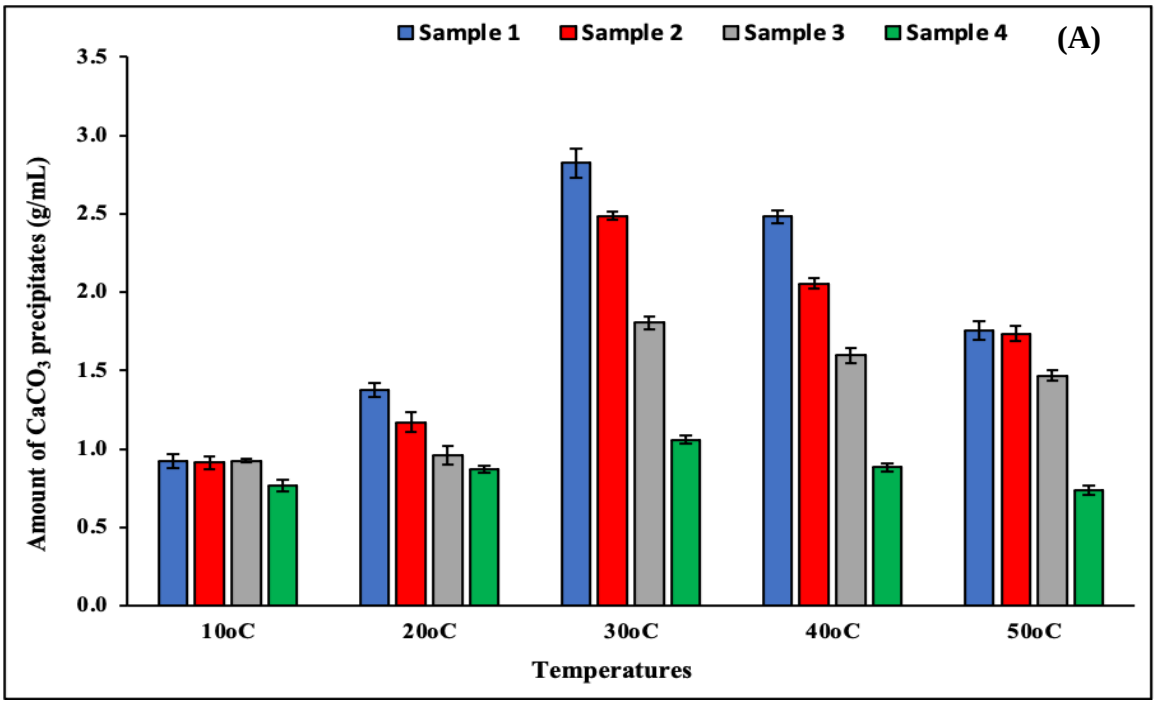

870

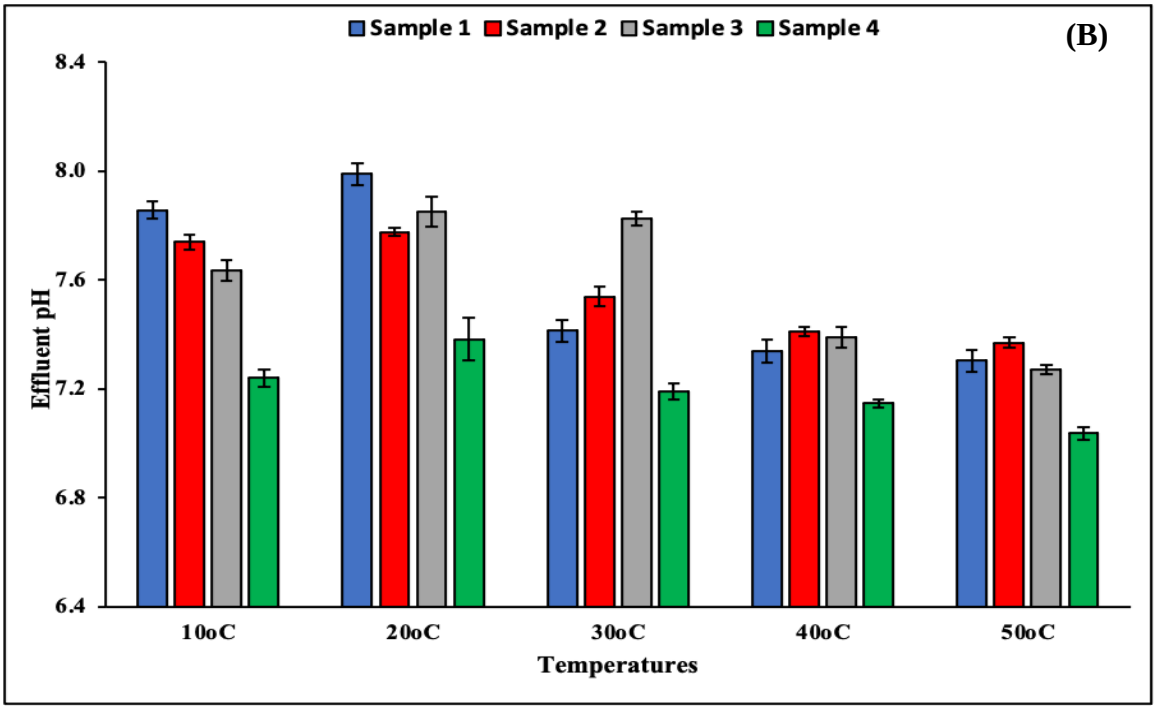

871

872 **Fig. 6:** Effect of different temperatures on treated specimens. (A) Mass of $CaCO_3$ contents, and (B) pH of the

873 effluent solutions. The error bars represent standard deviations.

874

875

876

877

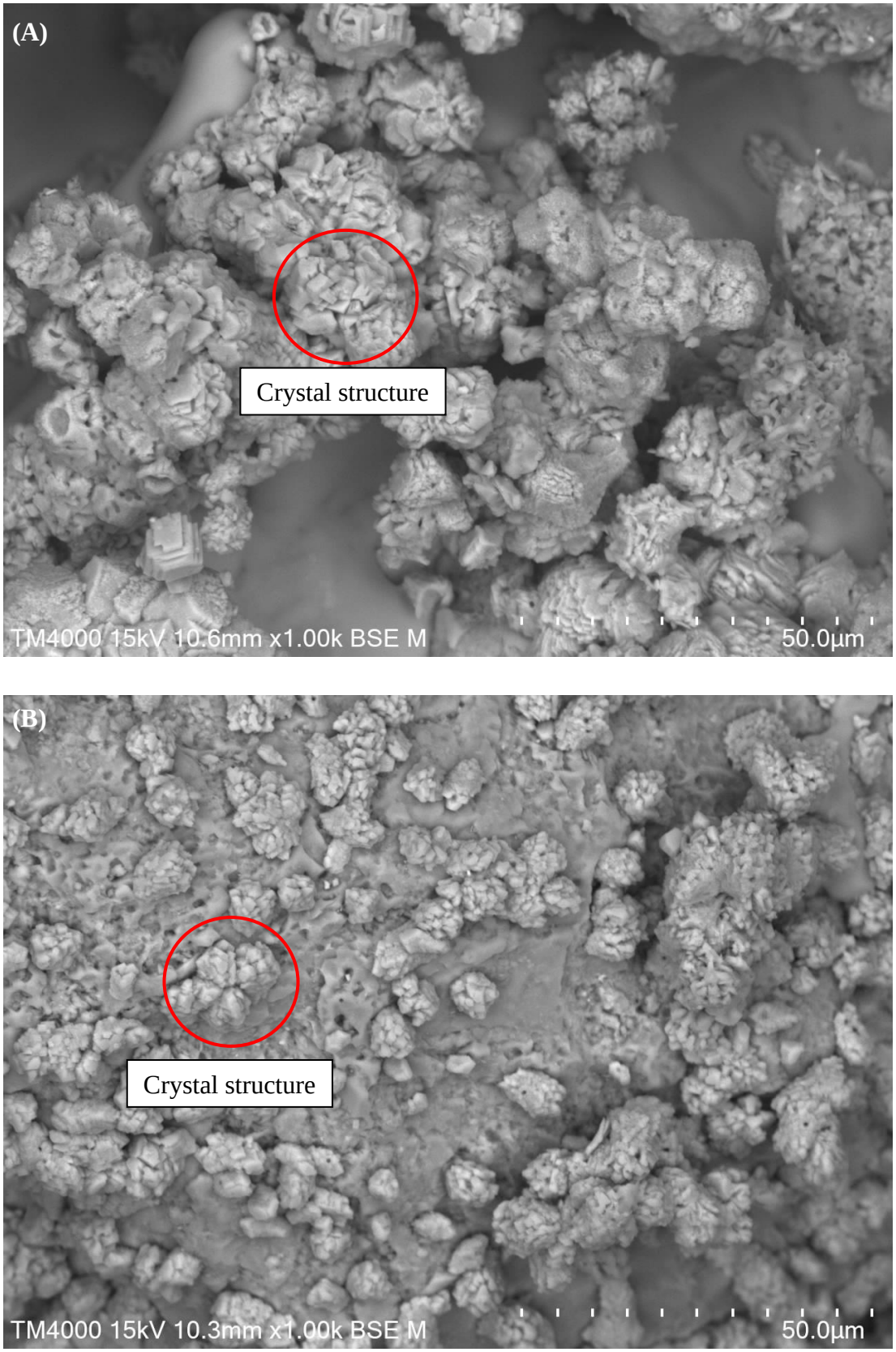

Fig. 7: SEM images showing the surface morphologies at 1000x magnifications of bio-treated soil particles with crystal formations after MICP treatment. (A) soil sample-1; (B) soil sample-2; (C) soil sample-3; and (D) soil sample-4.

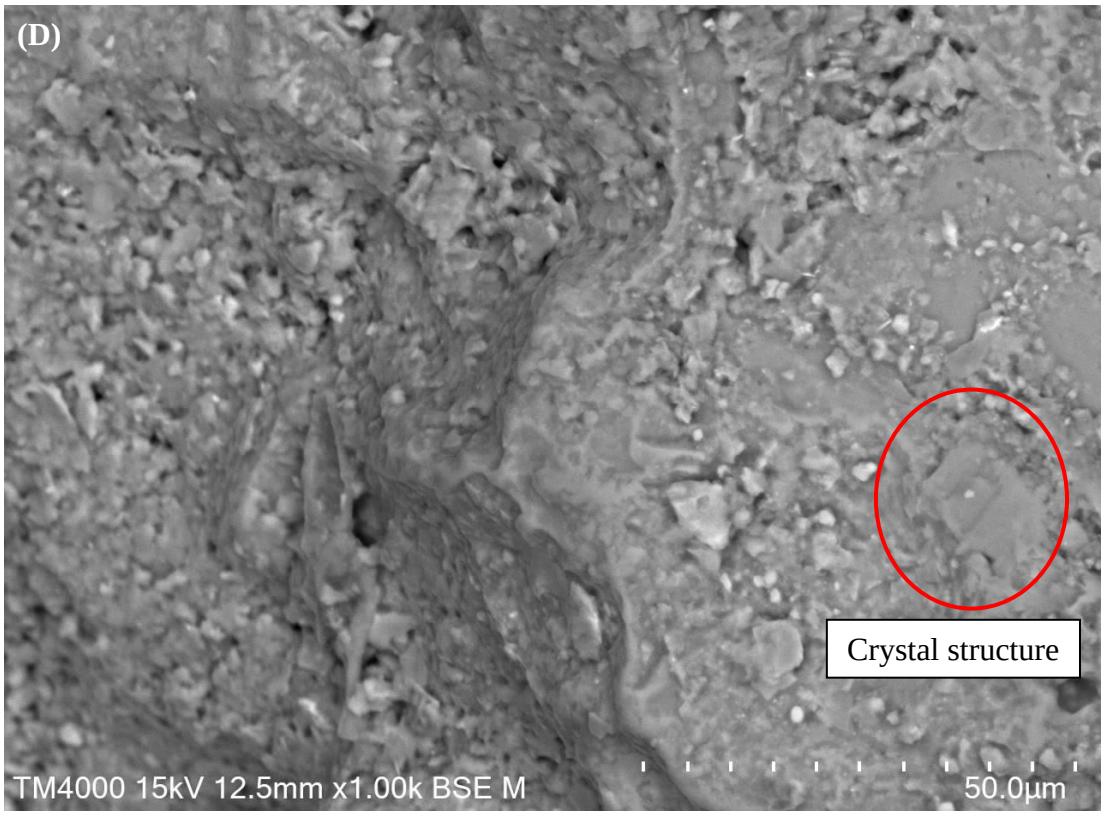

Fig. 7: continued.

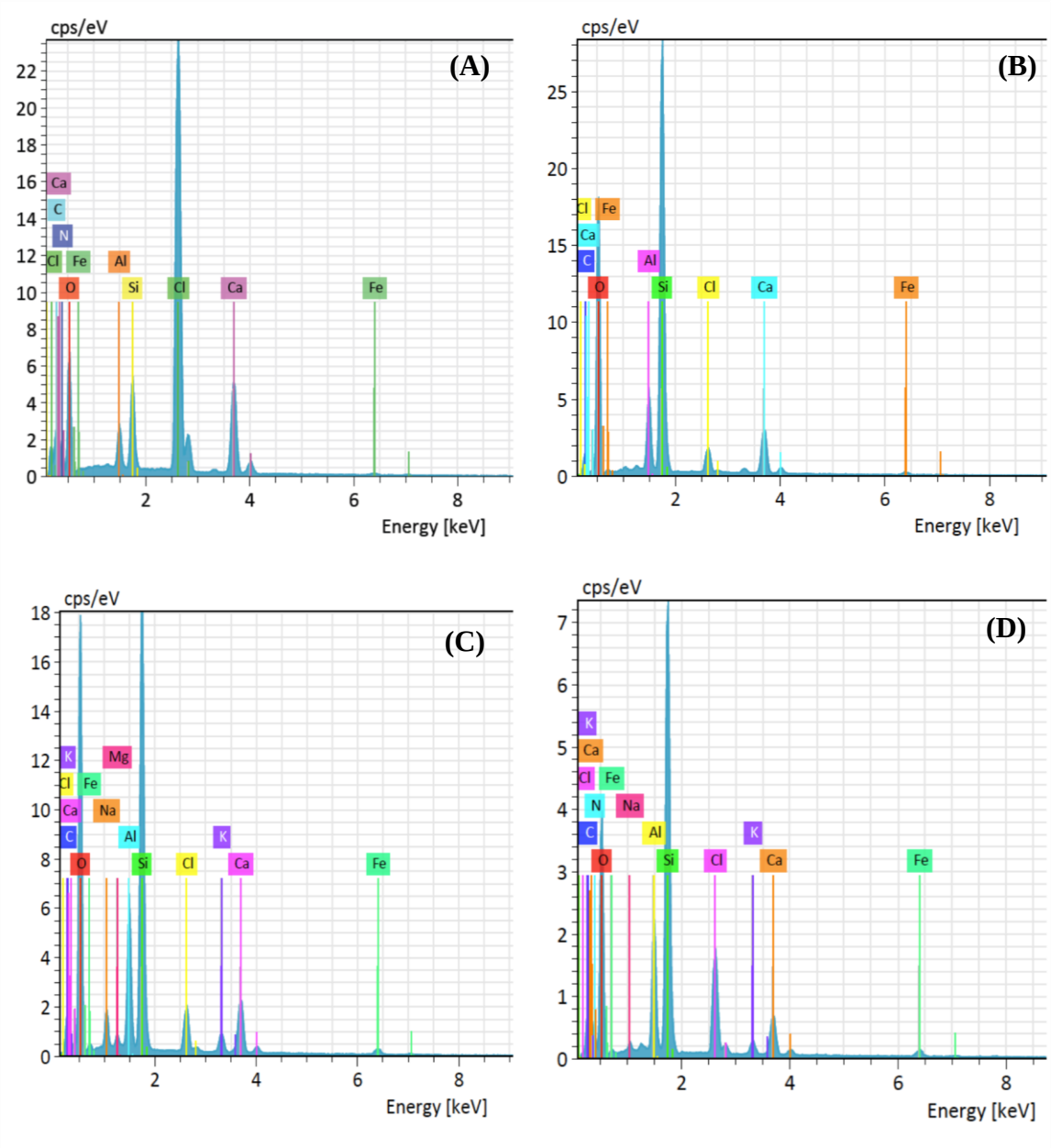

Fig. 8: EDS spectrum graphs for biocemented samples after being treated with cementation solution and ureolytic bacterial cultures cultivated with (A) medium 1, (B) medium 2, (C) medium 3, and (D) medium D.

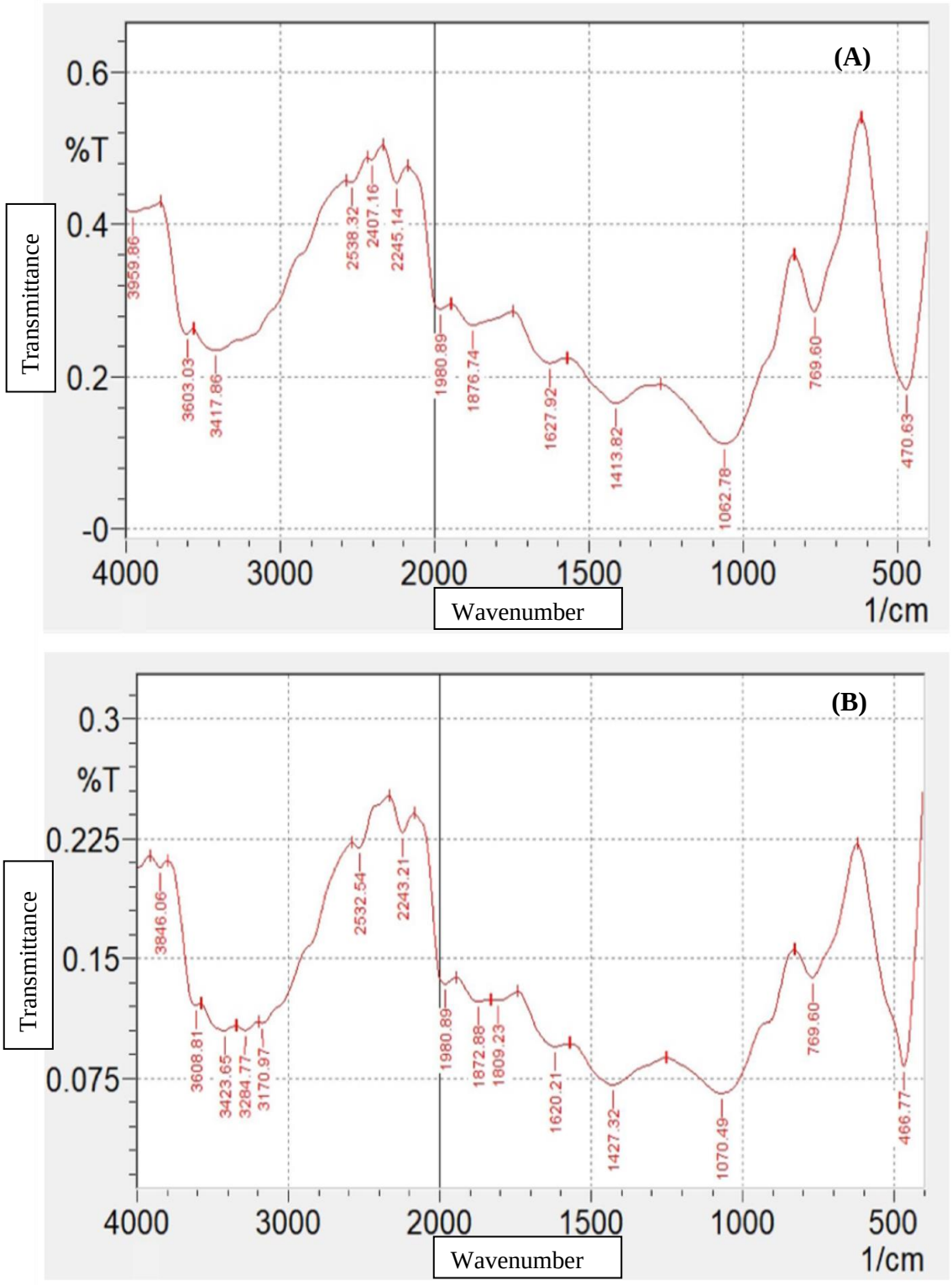

Fig. 9: The FTIR images of soil samples subjected to MICP treatment containing cementation solution and ureolytic bacterial cultures. (A) soil sample-1, (B) soil sample-2, (C) soil sample-3, and (D) soil sample-4.

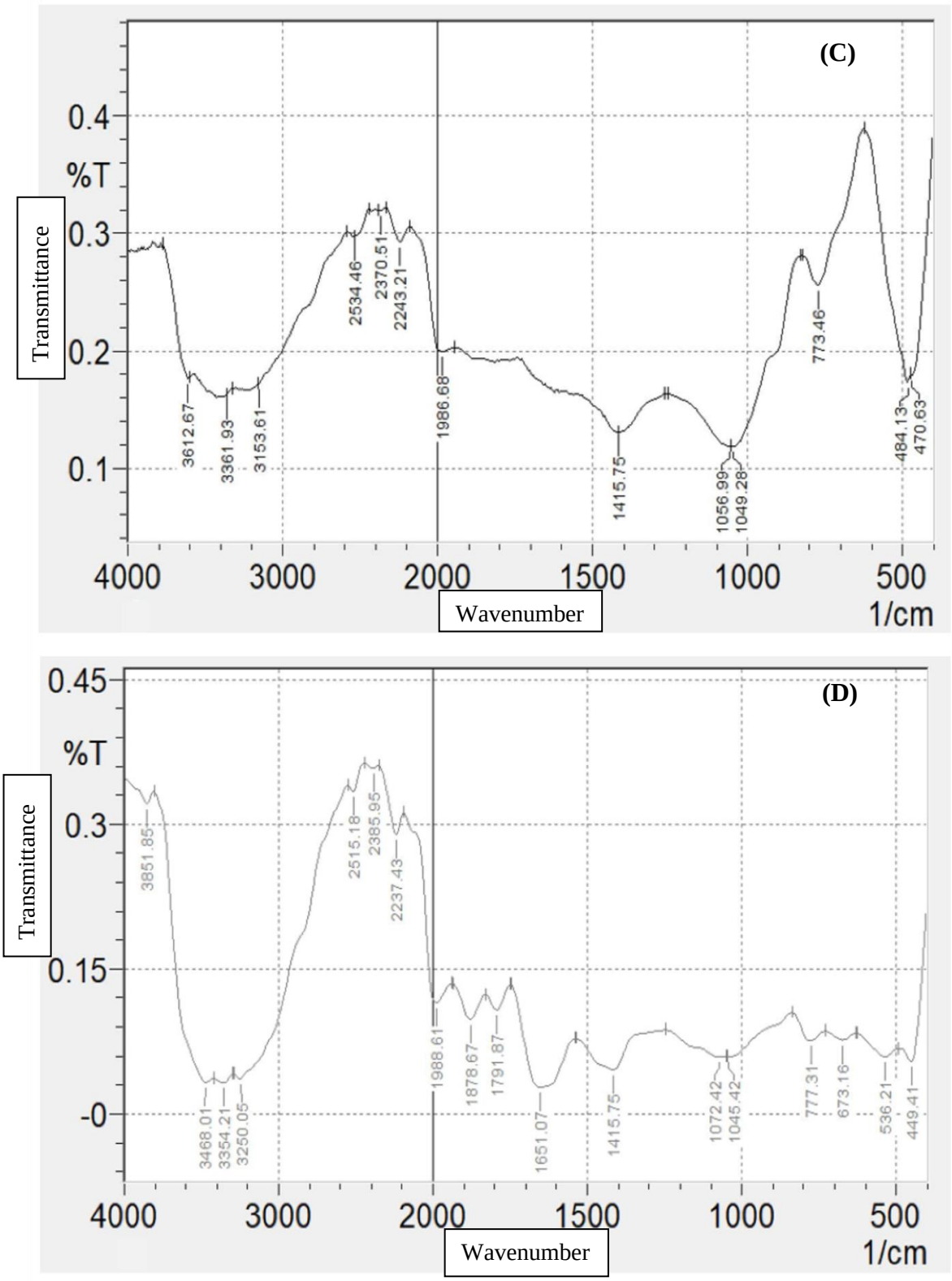

Fig. 9: continued.

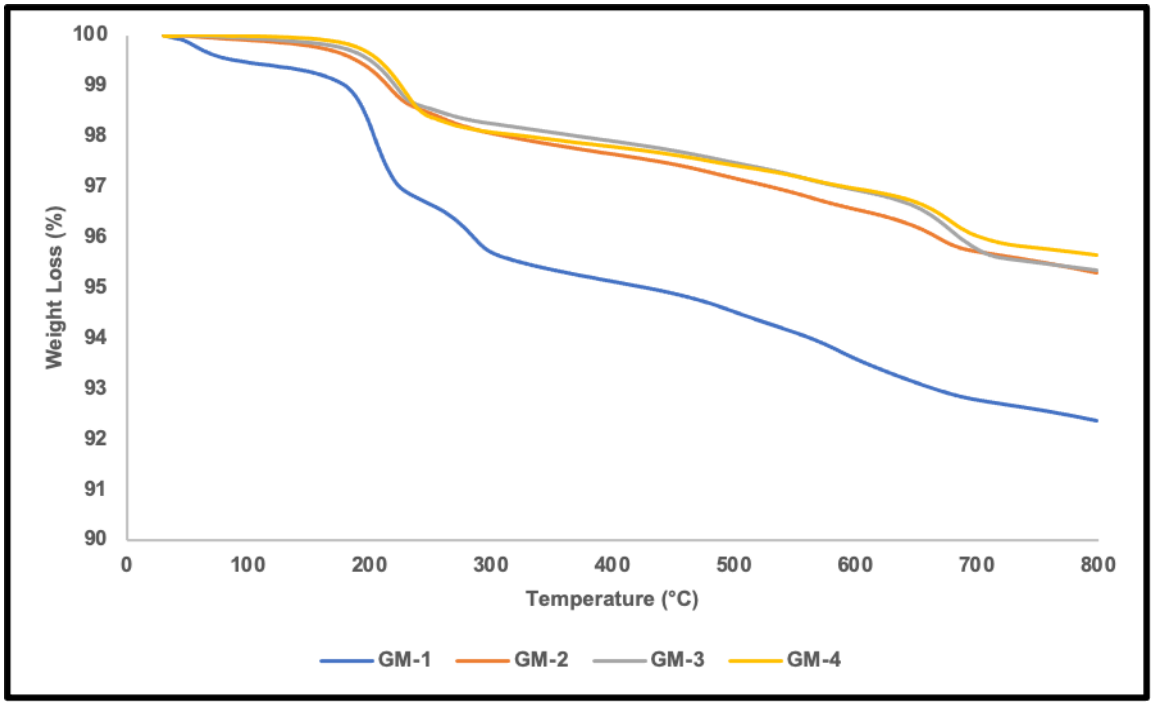

Fig. 10. TGA thermograph of soil sample-1 (GM-1), soil sample-2 (GM-2), soil sample-3 (GM-3), and soil sample-4 (GM-4).

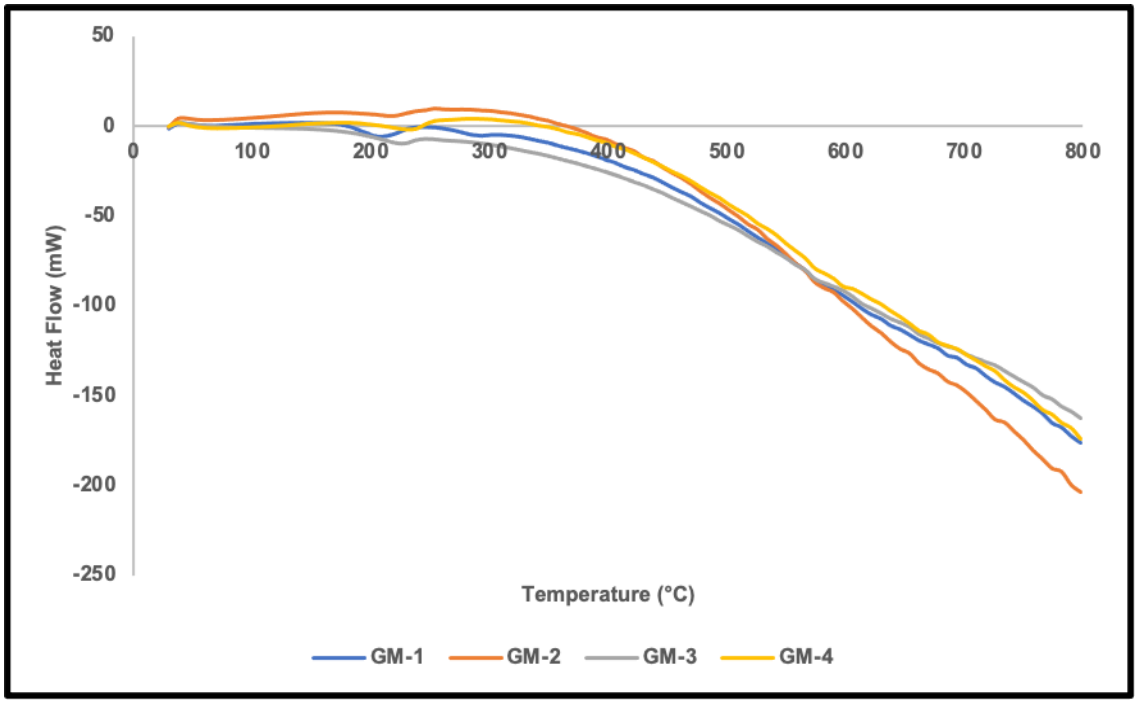

Fig. 11: DSC thermograph of soil sample-1 (GM-1), soil sample-2 (GM-2), soil sample-3 (GM-3), and soil sample-4 (GM-4).

List of tables

Table 1: Physiochemical properties of pelletized organic manure

Parameter	**Unit**	**Result**
pH	-	7.7
Electrical conductivity	µs/cm	4040.0
total nitrogen	%	0.3
carbon	%	2.6
organic nitrogen	%	0.2
phosphorous	%	0.2
chloride	mg/L	1278.0
aluminium	mg/L	45.3
calcium	%	0.2
copper	mg/L	5.8
iron	mg/kg	5.50
lead	mg/kg	4.1
magnesium	%	0.3
manganese	mg/kg	17.6
potassium	%	0.3
sodium	mg/kg	94.4
sulphur	mg/kg	22.1
zinc	mg/kg	5.2
moisture content	%	19.4
organic matter	%	39.1

926 **Table 2:** X-ray fluorescence analysis of pelletized organic manure

Chemical composition	**Mass content**
Silicon dioxide	40.15%
Calcium oxide	14.14%
Potassium oxide	7.14%
Aluminium oxide	7.35%
Phosphorus pentoxide	7.62%
Iron (III) oxide	5.07%
Chlorine	2.44%
Sulfur trioxide	5.55%
Magnesium oxide	2.85%
Sodium oxide	5.54%
Titanium dioxide	0.81%
Manganesec(II) oxide	0.32%
Zinc oxide	0.29%
Dysprosium oxide	0.12%
Lead (II) oxide	0.08%
Actinium	0.07%
Rubidium oxide	0.07%
Arsenic trioxide	0.08%
Bromine	0.05%
Strontium oxide	0.05%
Copper (II) oxide	0.05%
Zirconium	0.05%
Krypton	0.03%
Chromium oxide	0.04%
Yttrium oxide	0.04%

927

928 **Table 3:** Summary of soil particle size distribution and some physico-chemical characteristics

Characteristics	**Value**
Unified Soil Classification	SP
D10	0.125 mm
D50	0.210 mm
D60	0.240 mm
Coefficient of Uniformity (Cu)	1.92
Coefficient of Curvature (Cc)	1.20
Specific Gravity (Gs)	2.670 kg/m³
Maximum dry density (ρdmax)	1.640 Mg/m³
Minimum dry density (ρdmin)	1.27 Mg/m³
pH value	6.29

929

930

931

932 **Table 4:** Elemental compositions of biocemented soil samples using EDS analysis

Element	**Atom percentage (%)**			
	Sample 1	**Sample 2**	**Sample 3**	**Sample 4**
Oxygen	32.6	60.5	61.3	44.7
Silicon	2.1	15.9	12.2	11.2
Carbon	25.3	16.3	15.7	20.5
Nitrogen	24.5	0.0	0.0	15.1
Chlorine	10.7	1.1	1.3	2.5
Aluminium	0.2	2.8	3.8	3.3
Calcium	3.9	3.1	2.1	1.4
Iron	0.7	0.4	0.5	0.4
Potassium	0.0	0.0	0.7	0.4
Sodium	0.0	0.0	1.9	0.5
Magnesium	0.0	0.0	0.5	0.00

933